

2015

Correlation of Ultrasonographic Small Intestinal Wall Layering with Histology in Normal Dogs

Alexandre Benjamin Le Roux

Louisiana State University and Agricultural and Mechanical College

Follow this and additional works at: https://digitalcommons.lsu.edu/gradschool_theses



Part of the [Veterinary Medicine Commons](#)

Recommended Citation

Le Roux, Alexandre Benjamin, "Correlation of Ultrasonographic Small Intestinal Wall Layering with Histology in Normal Dogs" (2015). *LSU Master's Theses*. 1148.

https://digitalcommons.lsu.edu/gradschool_theses/1148

This Thesis is brought to you for free and open access by the Graduate School at LSU Digital Commons. It has been accepted for inclusion in LSU Master's Theses by an authorized graduate school editor of LSU Digital Commons. For more information, please contact gradetd@lsu.edu.

CORRELATION OF ULTRASONOGRAPHIC SMALL INTESTINAL WALL LAYERING WITH HISTOLOGY IN NORMAL DOGS

A Thesis

Submitted to the Graduate Faculty of the
Louisiana State University and
Agricultural and Mechanical College
in partial fulfillment of the
requirements for the degree of
Masters of Science

in

The School of Veterinary Medicine
through
The Department of Veterinary Clinical Sciences

by
Alexandre Benjamin Le Roux
DrMedVet, Ecole Nationale Vétérinaire de Nantes, 2006
May 2015

To my parents, my family and all my friends, for their continuous support...

ACKNOWLEDGMENTS

Foremost, I would like to express my deepest gratitude to the members of my committee, Drs. Lorrie Gaschen, Frederic Gaschen, Abbigail Granger and Nathalie Rademacher for the continuous support and guidance that they gave me through my residency and Master program research, as well as during the preparation of this manuscript.

My sincere thanks also goes to Dr. Nobuko Wakamatsu for performing all the histological analysis and reviewing them with me, as well as Michael Kearney and Dr. Hugues Beaufrère for performing the statistical analysis of this study.

Thank you to Alec Gaschen for creating some of the schematics used in this manuscript.

I would also like to thank the Hunting Retriever Club of Baton Rouge for funding this project, as well as General Electric Ultrasound for providing the portable ultrasound machine used during this study.

Thank you to the staff of the East Baton Rouge Shelter as well, for their help and care during my time at their institution.

Finally, I would more particularly like to thank Dr. Lorrie Gaschen for her invaluable guidance and mentorship during the four years that I spent at LSU and to make this project, and many more, possible. Thank you.

TABLE OF CONTENTS

ACKNOWLEDGMENTS	iii
LIST OF TABLES.....	v
LIST OF FIGURES	vi
ABSTRACT	vii
INTRODUCTION	1
CHAPTER I – REVIEW OF THE LITERATURE	3
I.1. Small Intestinal Histological Layers	3
I.1.a. General considerations	3
I.1.b. Mucosa	5
I.1.c. Submucosa	6
I.1.d. Muscularis or muscularis propria	6
I.1.e. Adventitia or serosa	7
I.1.f. Small intestinal histological layering segmental and age-related variation ...	7
I.2. Small Intestinal Ultrasonographic Layers	8
I.2.a. Interaction of ultrasound with matter	8
I.2.b. Intestinal layering in dogs - the 5-layer model	12
I.2.c. Advanced ultrasound imaging in human medicine - the 9-layer model	13
I.2.d. Small intestinal ultrasonographic layer alterations	14
I.3. Histological and Ultrasonographic Intestinal Layering Correlation	26
CHAPTER II – CORRELATION OF ULTRASONOGRAPHIC SMALL INTESTINAL WALL LAYERING WITH HISTOLOGY IN NORMAL DOGS	31
II.1. Materials and Methods	31
II.1.a. Ultrasonographic and histological image acquisition	31
II.1.b. Ultrasonographic and histological images review and mensuration	33
II.1.c. Statistical assessment	33
II.1.d. Subjective assessment	34
II.2. Results	34
II.2.a. Subjective assessment	36
II.2.b. Statistical assessment	40
II.3. Discussion	41
CONCLUSION	50
REFERENCES	51
APPENDIX – PERMISSIONS TO USE COPYRIGHTED MATERIAL	57
VITA	59

LIST OF TABLES

Table 1 – Attenuation coefficients of the rectal wall in cows.....	9
Table 2 – The five-layered gastrointestinal wall on ultrasound imaging.	28
Table 3 – The nine-layered gastrointestinal wall on EUS imaging.....	28
Table 4 – Mean \pm standard deviation (SD) and range values for thickness of the duodenal, jejunal and ileal wall layers measured ultrasonographically.	40
Table 5 – Mean \pm standard deviation (SD) and range values for thickness of the duodenal, jejunal and ileal wall layers measured histologically.	40
Table 6 – Wall thickness in different region of the gastrointestinal tract in 122 healthy persons measured with a 12MHz transducer.	47
Table 7 – Ileal wall layer thickness in 122 healthy persons measured with transabdominal ultrasound.	48

LIST OF FIGURES

Figure 1 – Overall histological organization of the digestive tube.....	3
Figure 2 – Histological transverse section showing the different small intestinal histological layers observed on a duodenal sample after hematoxylin and eosin stain.	4
Figure 3 – Principle of reflection in ultrasound.....	10
Figure 4 – Ultrasound refraction between two tissues of different acoustic impedances.	12
Figure 5 – The 5-layer model of small intestinal ultrasonographic layering in dogs.	13
Figure 6 – Schematic of the nine-layered gastrointestinal wall observed on endoscopic ultrasound (EUS) imaging in people.	14
Figure 7 – Small intestinal mucosal thinning in dogs with parvoviral infection.....	15
Figure 8 – Mucosal hyperechoic striations.....	17
Figure 9 – Mucosal hyperechoic speckles.....	18
Figure 10 – Hyperechoic mucosal stripe.....	19
Figure 11 – Mucosal fibrosis in cats.....	20
Figure 12 – Parallel hyperechoic mucosal line in dogs.....	22
Figure 13 – Duodenal submucosal layer thickening.	23
Figure 14 – Muscularis thickening in cats.....	25
Figure 15 – Relationship between histological and ultrasonographic intestinal wall layers.	27
Figure 16 – Principle of ultrasonographic axial resolution.	29
Figure 17 – Small intestinal loops ultrasonographic images acquisition.....	32
Figure 18 – Ultrasonographic measurements of the different small intestinal layers.....	33
Figure 19 – Jejunal altered histological sample.	35
Figure 20 – Crushed histological duodenal sample and mild submucosal layer detachment.	35
Figure 21 – Mucosal microfilaria in a dog.	36
Figure 22 - Ultrasonographic small intestinal mucosal layer dual echogenicity.....	37
Figure 23 – Degree of ultrasonographic small intestinal mucosal layer dual echogenicity depending on lacteal dilation.	38
Figure 24 – The hyperechoic muscularis layer interface.	39
Figure 25 – Ileal echogenic mucosal line and its correlation with enlarged Peyer’s patches.	39
Figure 26 - Examples of additional intestinal layers observed in clinical veterinary patients..	42
Figure 27 – Effects of interface echoes on ultrasound layering.	46

ABSTRACT

Five intestinal layers are commonly described ultrasonographically in dogs. However, current high-frequency endosonography allows the identification of 9 layers in people. The aim of this study was to describe *ex vivo* small intestinal layering in dogs and correlate ultrasonographic layering with histological layers. Our hypothesis was that, similar to findings in humans, discrepancies exist in thickness and visibility of intestinal layers between histology and ultrasound in dogs.

Twelve adult dogs were included in the study. They were euthanized for reasons unrelated to gastrointestinal disease, but extensive medical history was unavailable. Duodenum, jejunum and ileum samples were resected immediately after euthanasia. Ultrasonographic images were acquired post-mortem and two needles, pinned on each side of the sample, were used to denote where transverse images were acquired, and histological sections were obtained accordingly. Comparison of ultrasonographic and histological layer thicknesses was performed statistically and subjectively, and intestinal layer echogenicity as well as presence of additional ultrasonographic layers were evaluated and compared with histological findings.

No significant statistical differences were noted between the ultrasonographic and histological small intestinal layer thicknesses. In addition to the five established layers, an additional hyperechoic line was observed within the muscularis of all samples, and corresponded histologically to the interface between the longitudinal and circular smooth muscle fibers of the muscularis. In 4 ileum samples, an additional hyperechoic thin mucosal line was observed parallel to the submucosa, corresponding histologically to submucosal lymphoid follicle hyperplasia (Peyer's patches). Finally, a variably intense hyperechoic line was visible at the inner aspect of the mucosa of every sample. This ultrasonographic layer corresponded to the mucosal villi on histology, and its degree of hyperechogenicity was related to the degree of lacteal dilation observed histologically.

In contrary to our hypothesis, statistical differences between ultrasonographic and histological small intestinal layers were not shown. It was also established that additional intestinal ultrasonographic layers could be observed *ex vivo*. Some of these layers were

considered to be normal histological interfaces, such as the interface between the circular and longitudinal muscularis layers, while some were correlated with histopathological findings, such as mucosal lacteal dilation or submucosal lymphoid follicle hyperplasia.

INTRODUCTION

Gastrointestinal disease is one of the most common sources of morbidity in dogs and is usually inflammatory, infectious or neoplastic in origin. Ultrasonography is commonly used to examine the intestinal wall in dogs, with five established alternating hyperechoic and hypoechoic intestinal layers reported: a hyperechoic lumen/mucosal surface, a hypoechoic mucosa, a hyperechoic submucosa, a hypoechoic muscularis propria, and a hyperechoic serosa, which was first described in veterinary medicine in 1989, using transabdominal ultrasound.^{1, 2}

Alterations in intestinal wall thickness, wall layering and echogenicity on ultrasound examination are established descriptors of intestinal disease.^{3, 4} Ultrasonographic assessment of wall layering is not always sufficient to identify intestinal pathology non-invasively.^{1, 3-7} Mucosal hyperechoic striations and speckles have recently been described and may be associated with chronic enteropathies in dogs.⁸⁻¹⁰ Hyperechoic mucosal striations are thought to result from reflected ultrasound pulses from dilated lacteals,¹⁰ and to be associated with mucosal inflammation, lymphangiectasia and protein losing enteropathies.^{8, 10} Mucosal speckles have also been observed with intestinal inflammatory disease but their origin remains unclear, and they may represent focal accumulation of reflective substances in the mucosal crypts (e.g., mucus, cellular debris, protein, mineralized or fibrous tissue, or gas).⁸⁻¹¹ These ultrasonographic features could be of importance as non-invasive markers of underlying intestinal disease, but studies correlating their presence to histology are lacking. Also, the intestinal layers described in literature ultrasonographically are only assumed to correlate with the histological layers (mucosa, submucosa, muscularis propria and serosa), based on publications in people using antiquated ultrasound technology, but direct correlation of these ultrasonographic layers with histology has not been confirmed in dogs using high-resolution ultrasound equipment and software now available. In addition, histological and ultrasonographic correlation of the intestinal layers is controversial in human medicine, in that ultrasonographic layers have been proposed to be created by artifact-

induced reflective interfaces.^{12, 13} Furthermore, with recent advances in ultrasound technology, additional intestinal layers (such as the inner and outer muscle layers of the muscularis propria) have been described ultrasonographically in people,^{12, 14-16} but these findings have never been reported in veterinary medicine.

The goal of this study is to correlate the high-resolution ultrasonographic appearance of the wall layering of the small intestine in healthy dogs with histology. It is hypothesized that the currently accepted ultrasonographic appearance of the mucosa, submucosa, muscularis and serosa do not correlate with the histological layers, and that additional intestinal layer visualization, such as the inner circular and outer longitudinal layers of the muscularis propria can be observed, ex vivo, using a high-frequency transducer.

CHAPTER I – REVIEW OF THE LITERATURE

I.1. Small Intestinal Histological Layers

I.1.a. General considerations

The gastrointestinal tract is a functional unit for digestion of food with well-coordinated anatomical parts that have different functions, with the main purposes of the small intestine being enzymatic digestion, together with absorption of nutrients.^{15, 17, 18}

Histologically, the gastrointestinal wall is constituted of four major wall layers, as seen in Figure 1 and Figure 2:^{12, 15-18}

- the mucosa, which is the most inner and thickest layer, bordering the intestinal lumen, composed of an epithelium, lamina propria and muscularis mucosae, the latter being divided into two layers of muscular fibers: a thin inner layer of circular fibers and a thicker outer layer of longitudinal fibers
- the submucosa
- the muscularis propria, composed of a thicker inner layer of circular muscular fibers and a thinner outer layer of longitudinal muscular fibers
- and finally the most outer layer, the serosa (also called adventitia), with or without subserosal fat.

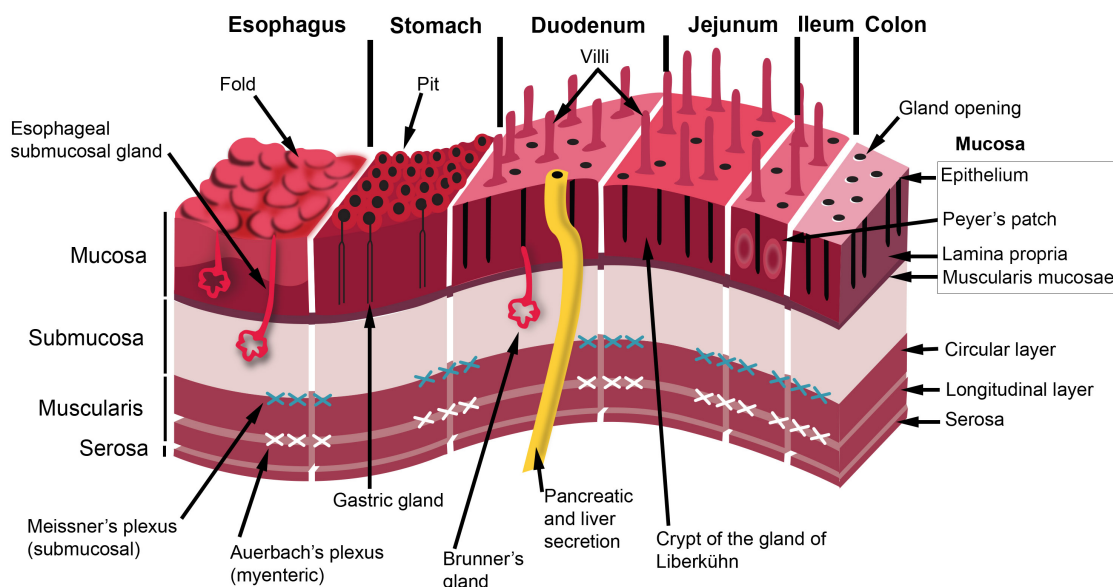


Figure 1 – Overall histological organization of the digestive tube.
(Adapted from¹⁵)

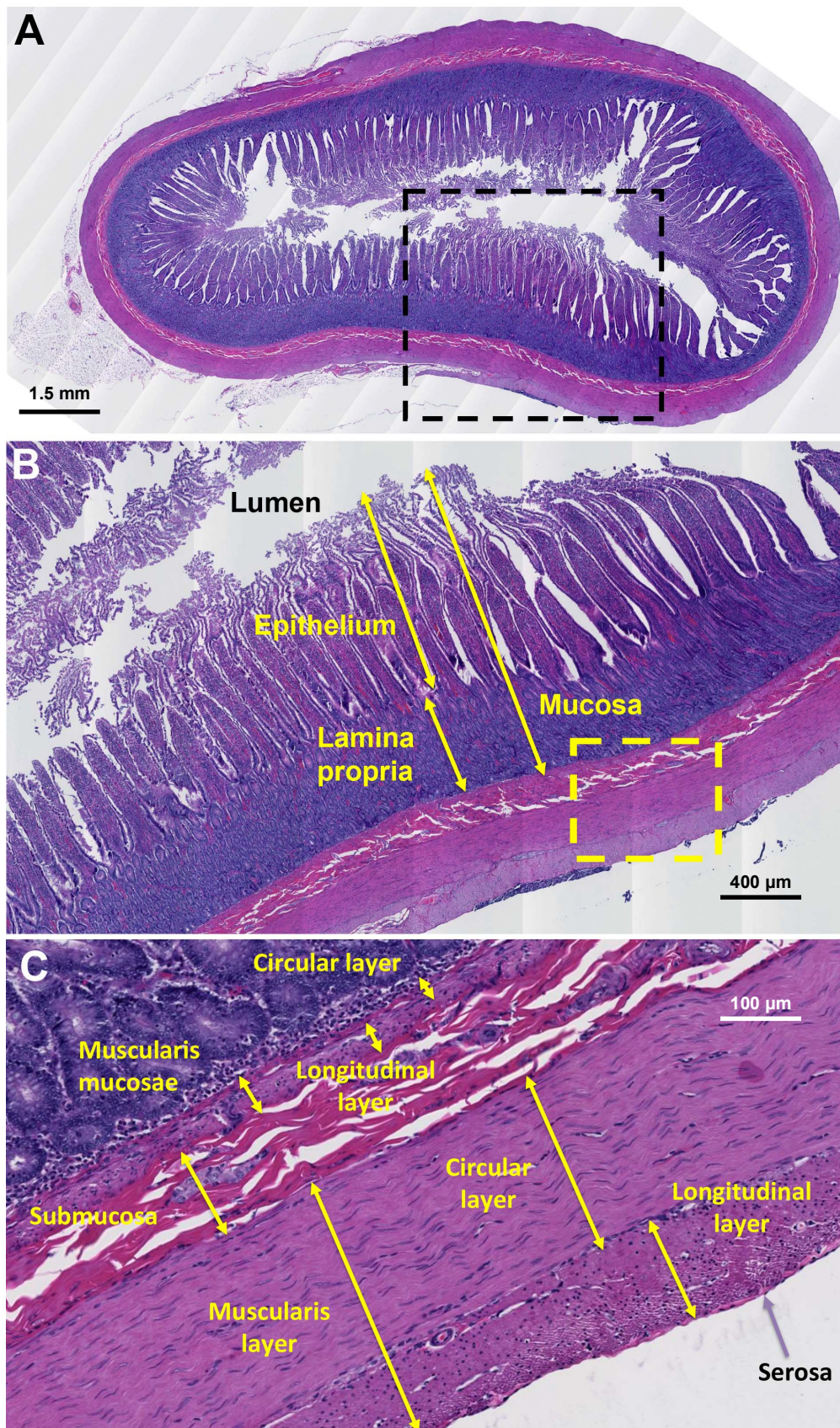


Figure 2 – Histological transverse section showing the different small intestinal histological layers observed on a duodenal sample after hematoxylin and eosin stain. The image (B) represents a magnified view of the duodenal wall at the level of the dotted black rectangle on image (A). The image (C) represents a magnified view of the outer part of the duodenal wall at the level of the dotted yellow rectangle on image (B).

I.1.b. Mucosa

The mucosa is the innermost intestinal layer, constituting the margins of the intestinal lumen, and is composed of a glandular epithelium, lamina propria, and muscularis mucosae (Figure 1 and Figure 2).^{17, 18} The epithelium of the mucosa has a very large surface, due to the formation of numerous villi protruding within the intestinal lumen. Each villus is lined by epithelial cells, which are themselves covered by microvilli, further increasing the surface where intestinal absorption can occur.¹⁶ The glandular epithelium also forms cylindrical structures, called crypts of Lieberkühn, containing enterocytes (absorptive epithelial cells), scattered goblet cells (mucus producing cells) and enteroendocrine cells, producing a wide variety of peptide hormones with local regulatory effects. At the base of these crypts, there are cells containing lysosome-rich granules (Paneth cells), which play a role in the maintenance of the gastrointestinal barrier and may also have growth and differentiation controlling functions on neighboring, local stem cells.^{17, 18}

The glandular epithelium is supported by the lamina propria, which is a layer of reticular connective tissue with elastin, reticulin, and collagen fibers, lymphocytes, plasma cells, and eosinophilic granulocytes, as well as lymphatics and capillaries.^{17, 18} Numerous and aggregated lymphoid follicles form the Peyer's patches, mostly present within the distal ileum in dogs.¹⁹⁻²¹ Altogether, the lymphoid cells of the lamina propria constitute the gut/mucosa-associated lymphoid tissue (GALT/MALT), which represents the intestinal mucosal immune system.¹⁷⁻¹⁹

Finally, the most outer part of the mucosa, the muscularis mucosae, consists of a thin layer of smooth muscle at the boundary of the mucosa and submucosa, observed throughout the digestive tract, from the esophagus to the colon, but absent in the anal canal.²² The type of smooth muscle is different between the esophagus and the rest of the gastro-intestinal tract, as the esophageal muscularis mucosae is only composed of longitudinal smooth muscles, while the gastric and intestinal muscularis mucosae is composed of an inner circular and an outer longitudinal smooth muscle layer.¹⁶⁻¹⁸ Despite its widespread distribution throughout the digestive tract, the physiological function of the muscularis mucosae seems to

be different than the one of the thicker muscularis propria, and is assumed to influence the absorptive and secretory functions of the epithelium, by inducing motion of the villi and emptying of the secreting glands of the mucosal intestinal crypts.^{22, 23}

I.1.c. Submucosa

The submucosa, between the muscularis mucosae and the muscularis propria (Figure 1 and Figure 2), is a fibrous connective tissue layer that contains fibroblasts, mast cells, blood and lymphatic vessels, and a plexus of nerve fibers, called the Meissner's plexus, composed of non-myelinated, postganglionic sympathetic fibers, and parasympathetic ganglion cells.¹⁵⁻¹⁸

In addition, the duodenal submucosa (and often the mucosal lamina propria as well) contains alkaline mucus-secreting acini, the Brunner's glands, which protect the mucosa against acid degradation from gastric fluid (Figure 1). In carnivores, these glands are limited to the proximal and mid-aspect of the duodenum.^{17, 18}

Finally the Peyer's patches, which represent aggregations of lymphoid follicles, are present in the mucosal lamina propria and submucosa of the small intestine, more particularly within the ileum.¹⁷⁻¹⁹

I.1.d. Muscularis or muscularis propria

The muscularis propria is mainly responsible of the propulsion of the food bolus through the gastrointestinal tract, by inducing circular and longitudinal contractions of the intestinal loops, and consists of two layers of smooth muscle (Figure 1 and Figure 2): an inner circular and an outer longitudinal layer, arranged in a helicoidal pattern.^{15, 17, 18, 23} A prominent nerve fiber plexus, the myenteric plexus, or Auerbach's plexus, is present between these two layers (Figure 1).¹⁵ Parasympathetic and postganglionic sympathetic fibers terminate in parasympathetic ganglion cells, and postganglionic parasympathetic fibers terminate in smooth muscle.^{17, 18}

I.1.e. Adventitia or serosa

The adventitia is the outermost layer of connective tissue composing the intestinal wall. It is called the serosa, when it is covered by a single layer of mesothelial cells.^{17, 18} In the gastrointestinal tract, the muscularis propria layer is bounded in most cases by serosa. Generally, the more freely movable parts of the digestive tract are covered by serosa, which function is to reduce friction, while the relatively rigidly fixed parts are covered by adventitia, which anchors and protects the surrounded organ.^{14, 17, 18, 24-26}

I.1.f. Small intestinal histological layering segmental and age-related variation

Several variations in the thickness of the different intestinal layers have been reported between the 3 segments of small intestine (duodenum, jejunum and ileum), as well as age-related thickness variations.^{17, 18, 27-29}

A progressive decrease in the thickness of the small intestinal wall has been reported from the duodenum to the distal jejunum, followed by a moderate increase throughout the ileum.^{18, 30} The mucosa in dogs is thickest in the duodenum, attributed to the size of the villi, the presence of duodenal glands, and the presence of lymphoid tissue in the lamina propria, while it is thinnest in the ileum, mainly due to the lower secretory activity and higher amount of lymphoid submucosal aggregates at this level.¹⁸ Within the jejunum, a progressive proximal-to-distal decrease thickness of the mucosa has been observed, likely due to the lack of intestinal glands and only minimum amount of lymphoid tissue in this segment.²⁹ The greatest thickness of the muscularis mucosae is also found in the duodenum, and is attributed to its function, as it induces motion of the epithelial villi and emptying of the secreting glands of the intestinal crypts, to promote enzymatic action on the chyme and increase contact between the epithelium and the luminal content. Finally, the muscularis propria has been reported to be the thickest in the distal ileum, which is probably related to the proximity of the ileal sphincter muscle, and to be the thinnest in the jejunum.^{29, 30}

In a recent study in dogs without gastrointestinal disease, continuous thickening of the jejunal layers has been reported, mainly during the first 10 years of life.³¹ The most significant changes have been detected in the lamina propria of the jejunal mucosa, where

the distance between the base of the crypts and the muscularis mucosae showed a strong correlation with the age of the dogs.³¹ Villus length and crypt depth did not show any clear relationship with age, but the whole mucosal thickness increased with aging. The thickness of the muscularis mucosae, submucosa and circular layer of the muscularis propria also increased with age, and for the muscularis mucosae and circular layer of the muscularis propria, this change displayed a stronger relationship in dogs less than 10 year-old.³¹ The longitudinal layer of the muscularis propria did not show any age-related changes. This increase in thickness of the muscular layer during lifetime has also been reported in the jejunum of rats.^{31, 32} A possible explanation might be an increased workload for the musculature, caused by a decrease in neuronal coordination as a result of neuronal cell loss during aging, which has been described in humans and rats.³¹ It is however not yet determined, if the increased muscular thickness is the result of a muscle fibers hypertrophy or if it is secondary to proliferation of connective tissue between the muscle fibers.^{32, 33}

I.2. Small Intestinal Ultrasonographic Layers

I.2.a. Interaction of ultrasound with matter

A basic understanding of ultrasonographic image formation is important to understand the origin of the intestinal layering observed ultrasonographically. Visible intestinal layers are visualized as a result of echo formation from the transmitted ultrasound beam. Echoes are produced by the interaction of the ultrasound beam with the tissue itself, where alterations in the density and speed of sound at an interface creates a reflection of sound that returns to the ultrasound transducer.¹⁶

The frequency of the ultrasound pulse produced by the ultrasound transducer plays an important role in both the depth of penetration of the ultrasound pulse and the resulting image resolution. In general, the higher the frequency, the lower the depth of penetration, and the higher the resolution. As an ultrasound pulse propagates through tissue, it can interact with it via absorption, scattering, reflection and refraction.^{33, 34}

I.2.a.i. Attenuation

Attenuation is due to scattering and absorption of the ultrasound pulse within the tissue traversed. The attenuation coefficient (α) is a function of frequency and can be experimentally determined. It is proportional to the path length of the ultrasound pulse and its frequency and for soft-tissue, its value is commonly considered to be equal to 1 dB per cm of path length per MHz.^{33, 34} In air and in bone, the attenuation is much higher, as a marked alteration in speed of sound and tissue density occurs as sound travels from soft tissues to these media. As a result, there is basically no transmission of ultrasound to interact with deeper structures through either gas or bone.³⁵ In water and most fluids, the attenuation is small, but increases as the square of the frequency increases (however remaining negligible). Therefore, only minimal attenuation is present in water and other fluids (hence low scattering), facilitating distinction between solid tissue and fluids in the ultrasonographic images.³³⁻³⁵ The only reported experimental measurements of ultrasound attenuation in the gastrointestinal tract have been performed on the rectal wall of cows (Table 1).³⁶

Table 1 – Attenuation coefficients of the rectal wall in cows.
(From³⁶)

Frequency (MHz)	Attenuation (dB/cm)
1	0.6
3	1.6
5	2.4

Absorbed ultrasound pulse energy in tissue traversed by the ultrasound beam is converted into:³³⁻³⁵

- cavitation (formation of micro bubbles of gas, occurring at high power levels, much higher than the one used in clinical equipment)
- heat (possible, but not noticed with clinical equipment)
- other unknown or unproven effects

Scattering occurs when the ultrasound pulse interacts with particles that are similar or smaller in size than the wavelength of the ultrasound pulse and have different impedance values than the propagating medium.³³ These particles are also termed non-specular reflectors. Scattering occurs in inhomogeneous media, such as tissue. For instance, tissue

containing fat or collagen scatters ultrasound to a greater degree than other tissues, resulting in a hyperechoic appearance of fat or fibrous tissue ultrasonographically.^{16, 37} In medical imaging, the size of the organs assessed is much larger than the wavelength of the ultrasound pulse.^{33, 35} Therefore, if the organ has a large, smooth surface for sound to reflect from, it can create an echo that can be described. Such reflections are called specular reflections, and are much like reflection of light off a mirror.^{33, 35}

I.2.a.ii. Reflection

Just as with a sonar, a portion of the ultrasound beam emitted by the ultrasound transducer through the tissue assessed is reflected at tissue interfaces. The reflected beam will be detected if it returns to the transducer that generated it.^{33, 35} If the ultrasound beam is perpendicular to the interface (called normal incidence), or close to it, some of it will be reflected back toward the transducer, while the rest will be transmitted across the interface (Figure 3).¹⁶ If the reflected ultrasound reaches the transducer and is measured, it is called an echo, and its amplitude is measured and used to create an image.^{16, 33-35}

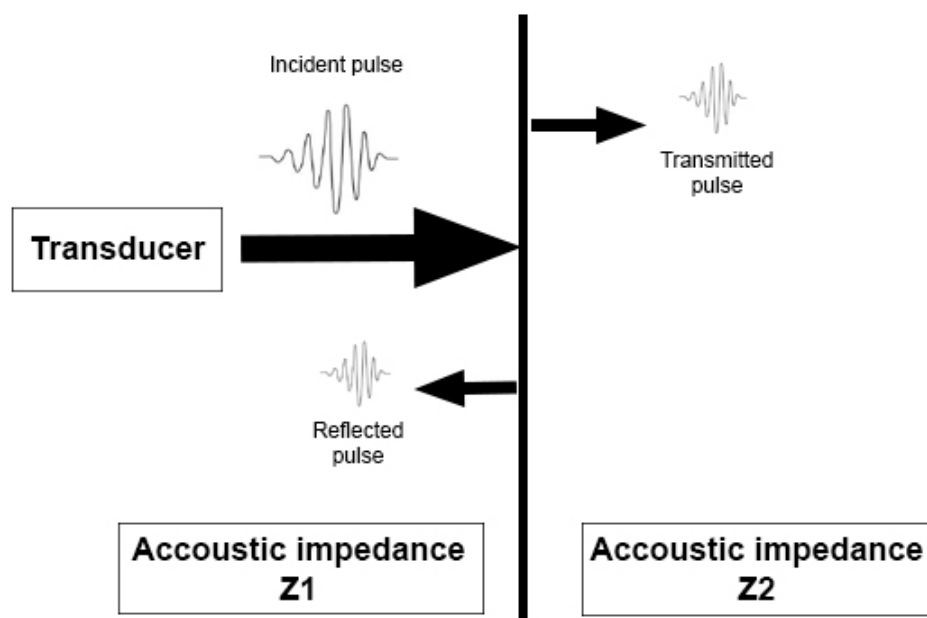


Figure 3 – Principle of reflection in ultrasound.
An incident ultrasound pulse generated by a transducer will be partially reflected at interfaces between two tissues with different acoustic impedances. The percentage reflected and transmitted is dependent on the difference in acoustic impedance between the two tissues. (Adapted from¹⁶)

The concept of reflection is important to understand, since this property is partially responsible for the layered appearance of the gastrointestinal wall on the ultrasound images.¹⁶ Reflection occurs when an ultrasound pulse encounters an interface between two large structures, relative to the wavelength of the ultrasound beam, with different acoustic impedance values. These interfaces are also termed specular reflectors.^{16, 33-35} The acoustic impedance (Z) of tissue is related to the change in acoustic velocity (c) and density (ρ) between interfaces of the tissue by the following equation:³³⁻³⁵

$$Z = \rho \cdot c$$

The percentage of the incident ultrasound beam reflected from the interface of two tissue layers with acoustic impedances of Z_1 and Z_2 is given by the following equation:³³⁻³⁵

$$\text{Fraction reflected} = \text{reflectance} = \left[\frac{(Z_1 - Z_2)}{(Z_1 + Z_2)} \right]^2$$

This percentage tends to be approximately 1% for reflection from different soft-tissue interfaces, and approximately 50% for soft-tissue to bone interfaces, and therefore air/tissue and bone/tissue interfaces reflect virtually all the ultrasound beam that strikes them, while other organic tissues show various patterns of reflection that are much reduced in comparison. Organs such as the liver, kidney, pancreas, and spleen have an internal structure, producing echoes and giving their internal anatomy a speckled pattern (called texture) on the resulting ultrasonographic images.^{15, 16} Fluid-filled structures, such as the urinary bladder or cysts, have no internal structure or alteration in density and speed of sound and thus minimal texture. This makes ultrasound valuable in distinguishing between cysts and solid structures.

The layered structures visualized in an ultrasonographic image are a combination of the echoes generated by specular reflectors that result from the acoustic impedance differences between tissue layers, and the non-specular reflectors within each tissue layer, creating the echogenic texture of the tissue layer.¹⁶ For instance, the hyperechogenicity of the submucosa and serosa is the result of scattering from non-specular reflectors, presumably due to the relatively high collagen and fat content of these layers.¹⁵

I.2.a.iii. Refraction

If the incident beam is not perpendicular to the interface (oblique incidence) between two tissues of different impedance, then the reflected beam will not return along its incidence path to the ultrasound transducer, but rather be deviated at an angle of reflection equaling the angle of incidence (Figure 4). The transmitted ultrasound beam, called the refracted beam, will also be deviated to a new direction, given by the angle of refraction.³³⁻³⁵

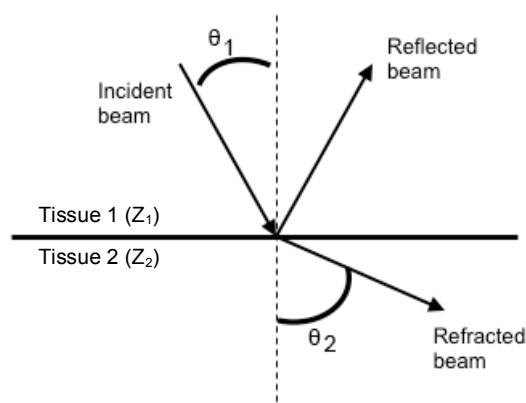


Figure 4 – Ultrasound refraction between two tissues of different acoustic impedances. θ_1 : incident angle in first material; θ_2 : refracted angle in second material. (Adapted from³³)

The refraction angle and relative intensities of the reflected and refracted beams depends upon the angle of incidence, as well as the impedances of the two tissues at the interface.³³⁻³⁵ Frequency is still the same in both media, but both wavelength and direction are changed. If this refracted beam is later reflected back to the transducer and measured as an echo, it will blur the image in exactly the same way as scatter blurs an X-ray image.³³⁻³⁵

I.2.b. Intestinal layering in dogs - the 5-layer model

In dogs, a five-layered appearance of the intestinal wall has been reported, with alternating hyperechoic and hypoechoic layers (Figure 5):^{1, 3, 4, 6, 38}

- An inner hyperechoic layer, representing the interface between the intraluminal content or empty lumen and the epithelium of the intestinal mucosa
- a hypoechoic layer, representing the rest of the intestinal mucosa
- a hyperechoic layer, mostly due to the submucosa
- a hypoechoic layer, mostly due to the muscularis layer
- an outer hyperechoic thin layer, mostly due to the serosa.

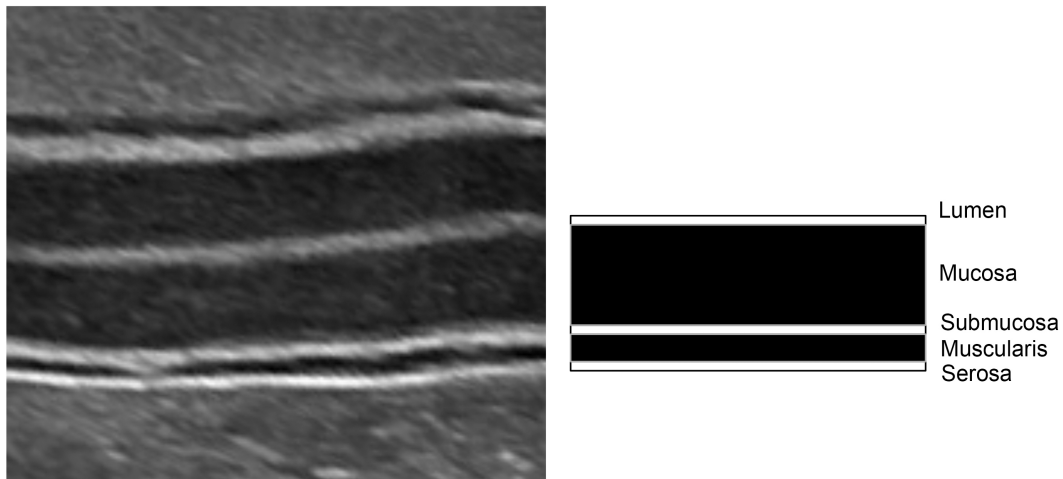


Figure 5 – The 5-layer model of small intestinal ultrasonographic layering in dogs. Longitudinal ultrasonographic image of the duodenum of a healthy dog on the left, and its schematic representation showing the different layers visualized on ultrasound.

I.2.c. Advanced ultrasound imaging in human medicine - the 9-layer model

With the development of endoscopic ultrasound (EUS) and the use of higher frequency transducers (20-MHz ultrasonographic probes or higher) in people, additional layers have been described in the normal gastrointestinal wall, and a nine-layer small intestinal wall layering model is currently reported when using endoscopic ultrasound imaging (Figure 6).^{12-16, 25, 38-46}

Standard echoendoscopes use ultrasound frequencies between 5 and 12 MHz.^{14, 47} Despite closer contact with the adjacent small intestinal wall, the first echoendoscopes had a relatively low resolution. A significant advance in endoscopic ultrasound came with the development of catheter ultrasound probes or miniproboscopes, which can be passed through the operating channel of standard endoscopes, with frequencies ranging between 7.5 and 20 MHz, providing higher resolution of structures within 1–2 cm of the transducer, and therefore allowing visualization of additional layers within the gastrointestinal tract.^{14, 47}

Using this imaging modality in humans, an additional hyperechoic line has been reported in the middle of the fourth hypoechoic layer (the ultrasonographic muscularis layer), which is observed ultrasonographically as an interface echo due to the difference of impedance between the inner circular and outer longitudinal muscular fiber layers of the muscularis propria, as well as secondary to the presence of fibrous tissue and myenteric plexus present between these two muscle layers (Figure 6).^{7-11, 39}



Figure 6 – Schematic of the nine-layered gastrointestinal wall observed on endoscopic ultrasound (EUS) imaging in people.

Schematic representation showing the different layers visualized on endoscopic intraluminal ultrasonographic images of a normal small intestinal loop. (1) Epithelial interface; (2) epithelium; (3) lamina propria plus acoustic interface between lamina propria and muscularis mucosae; (4) muscularis mucosae minus acoustic interface between lamina propria and muscularis mucosa; (5) submucosa plus acoustic interface between submucosa and inner muscularis propria; (6) inner muscularis propria minus interface between submucosa and inner muscularis propria; (7) fibrous tissue band separating inner and outer muscularis propria; (8) outer muscularis propria; (9) serosa and serosal fat. (Adapted from¹⁶)

The muscularis mucosae can also be distinguished as a separate layer when it is thickened and/or when high-frequency transducers are used. In this situation, there are actually two additional layers at the outer aspect of the mucosal layer: a hyperechoic line at the inner aspect of the mucosa, due to the interface of the lamina propria and the muscularis mucosae, and an outer hypoechoic layer from the muscularis mucosae itself.^{13, 15, 48}

I.2.d. Small intestinal ultrasonographic layer alterations

Ultrasonographic alterations of the small intestinal layering, including additional layers (in comparison to the reported 5 or 9-layer models), changes of echogenicity and/or thickness of the layers, have been reported in both veterinary and human medicine. In this part, only conditions inducing modifications of the thickness and/or echogenicity of the intestinal wall layers (without loss of the intestinal layering) will be reviewed. Intestinal diseases inducing loss of the intestinal wall layering (such as neoplasia or severe infectious diseases) will not be evaluated.

I.2.d.i. Mucosal thinning

Mild-to-moderate small intestinal wall thickening without loss of layering has been reported with enteritis.⁷ However, in some inflammatory or infectious diseases, the small

intestinal wall layers can be significantly affected or even completely lost, and decreased or absent peristalsis is often present.^{3, 4, 6, 7, 49} In parvoviral infection for instance, the canine parvovirus exhibits a tropism for rapidly replicating cell populations of the intestinal crypt epithelium, lymphoid, and hematopoietic tissues.^{9, 50, 51} In a study performed in 40 puppies between 6 and 24 weeks of age with confirmed canine parvoviral enteritis,⁹ ultrasonographic changes revealed fluid-filled, atonic small and large intestines, duodenal and jejunal mucosal layer thinning with or without indistinct wall layers and irregular luminal–mucosal surfaces, extensive duodenal and/or jejunal hyperechoic mucosal speckling, and small intestinal corrugation (Figure 7).

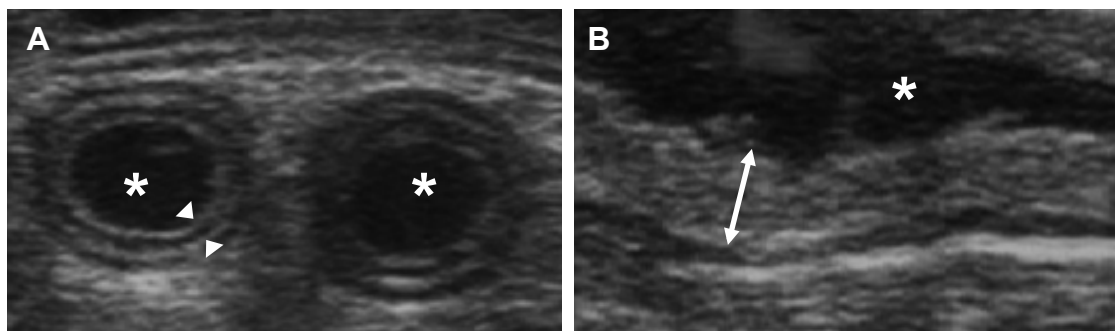


Figure 7 – Small intestinal mucosal thinning in dogs with parvoviral infection. (A) Transverse fluid-filled jejunal loops, with indistinct wall layering, and thinner mucosal layer. The thin mucosa is visible between the two white arrowheads. The white asterisks mark the dilated lumen of the jejunal loops. (B) Magnified longitudinal image of the far wall of the descending duodenum of a dog with parvoviral enteritis, showing severely hyperechoic mucosal layer (marked by the double arrowhead line), irregularity and mild undulation of the luminal–mucosal interface, likely due to severe villi necrosis and/or dilated intestinal glands, filled with necrotic debris. The fluid-dilated intestinal lumen is marked by the white asterisk. (Adapted from⁹, permission to reuse in Appendix)

These ultrasonographic changes were attributed to the mode of propagation of the parvovirus.⁹ This virus is acquired by a fecal–oral route of transmission and then reaches the intestinal mucosa hematogenously, replicating in the epithelium of intestinal crypts, where viral proliferation causes extensive epithelial necrosis, villus blunting and atrophy, disruption of the lamina propria, with mucosal thinning, erosion/ulceration and dilated intestinal glands, filled with necrotic debris, also commonly observed.^{9, 50, 51}

I.2.d.ii. Intestinal wall thickening

Intestinal wall thickening can also be observed ultrasonographically, and is commonly associated with inflammatory bowel disease or neoplasia, but also reported with diffuse edema, secondary to hypoalbuminemia, congestive heart failure, or vascular abnormalities for instance.^{3, 4, 52} The distribution of the wall thickening may sometimes be helpful to differentiate benign and neoplastic diseases, with benign lesions usually presenting with more diffuse mild-to-moderate wall thickening and conservation of the intestinal layering, while neoplastic lesions usually lead to more severe focal thickening or mass lesions, with disruption or loss of the intestinal wall layers (with the exception of some round cell tumors, more especially lymphoma).^{3, 4, 7, 52, 53} However, normal findings during an ultrasound examination do not completely rule out intestinal disease, as dogs with confirmed intestinal inflammation may have no detectable ultrasonographic intestinal wall thickening. In a recent study in dogs with confirmed inflammatory bowel disease,⁵² a correlation between intestinal wall thickness and histological diagnosis or response to treatment was not found. This may have been due to a variable degree of thickening of the small intestine throughout the intestinal tract (with some segments affected more than others), an insufficient amount of infiltrating cells to induce intestinal wall thickening but significant enough to result in clinical signs, measurement errors due to the difficulty to assess the full intestinal wall thickness (maybe due to variable amount of peri-intestinal fat or variations in applied pressure during the abdominal ultrasound) or finally, villus atrophy accompanying inflammation, possibly resulting in decreased wall thickness. Therefore, measurements of the intestinal wall thickness interpreted on their own do not appear reliable to establish a diagnosis of intestinal inflammation, and may even result in a false negative diagnosis in some cases of inflammatory bowel disease.⁵²

I.2.d.iii. Hyperechoic mucosal speckles, striations and mucosal stripe

Intestinal wall thickness is a well-described criterion of evaluation of inflammatory bowel disease in humans,⁵⁴⁻⁵⁸ but in dogs, it appears that measurement of bowel wall thickness has not been proved to be either sensitive or specific for the presence, type, and

severity of intestinal disease.^{7, 8, 52, 59} The echogenicity of the small intestinal mucosa and the presence of secondary abnormalities of the intestine and contiguous organs (such as effusion, or lymphadenopathy for instance) may be more helpful for detecting and differentiating causes of chronic inflammatory bowel disease.⁸ Different patterns of increased mucosal echogenicity have been recently reported in several studies in dogs: hyperechoic speckles, hyperechoic striations and a mucosal hyperechoic stripe.^{5, 8, 10, 11, 59, 60} Hyperechoic speckles have been observed as hyperechoic foci disseminated throughout the small intestinal mucosal layer, while mucosal striations are observed as multiple thin hyperechoic lines within the mucosal layer, extending between the mucosa–lumen interface towards the submucosal layer, and the hyperechoic stripe, as a hyperechoic line thicker than the mucosa–lumen interface, or as a thick rounded focus on either side of the plicated intestinal lumen/mucosa.^{3-5, 8, 10, 11, 59, 61}

In recent studies, hyperechoic mucosal striations (Figure 8) have been associated histologically with lacteal dilation in 96% of dogs, and clinically with protein losing enteropathy in 78% dogs,^{8, 10, 61} and are thought to result from reflected ultrasound pulses from dilated lacteals, characteristic of lymphangiectasia, containing intraluminal reflective substances including lipid, cellular debris, protein, fibrous tissue, gas, mineral, or mucus.^{8, 10, 60}

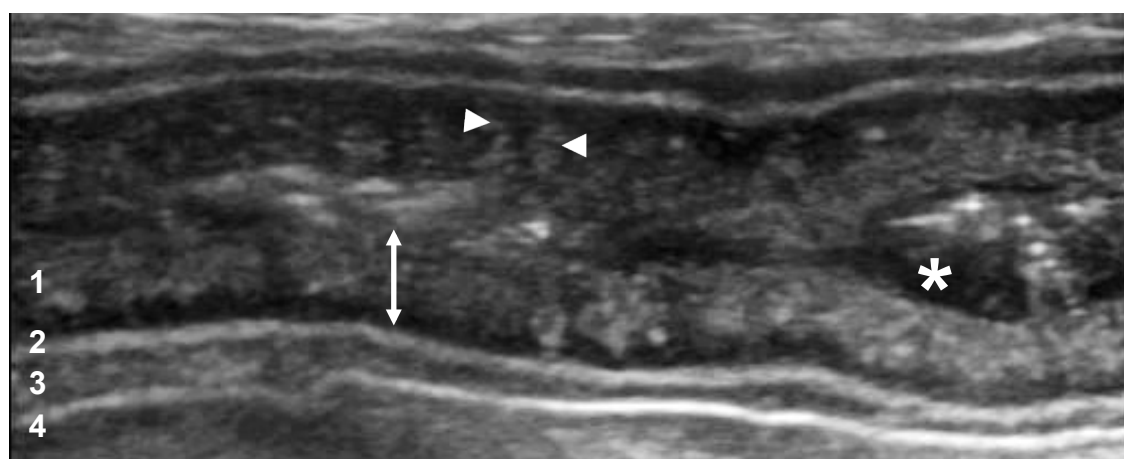


Figure 8 – Mucosal hyperechoic striations. Longitudinal ultrasonographic image of the duodenum of a dog, diagnosed with lymphangiectasia, showing ill-defined parallel mucosal hyperechoic lines (white arrowheads) extending from the lumen-mucosa interface towards the submucosal layer (double arrowhead line). The gas and fluid-dilated intestinal lumen is marked by the white asterisk. (1) Mucosa; (2) submucosa; (3) muscularis propria; (4) serosa.

Concurrent inflammation is a concomitant feature associated with lacteal dilation in dogs diagnosed with lymphangiectasia, with a mild-to-moderate inflammatory infiltration, including various proportions of lymphocytes, eosinophils, plasma cells, and neutrophils, present in 88 to 91% of dogs.^{10, 59}

Hyperechoic mucosal speckles (Figure 9) are considered a less-specific finding. They have been observed in 70% of dogs with mucosal striations and are speculated to represent a partial section through part of dilated lacteals, or focal accumulation of mucus, cellular debris, protein, or gas in the mucosal crypts.^{2, 8, 60} Their clinical significance is not clearly known, their presence is not limited to dogs with lymphangiectasia and they have also been observed independently, without mucosal striations. A direct connection between their visualization and the ingestion of a fatty meal has not been established.⁶⁰

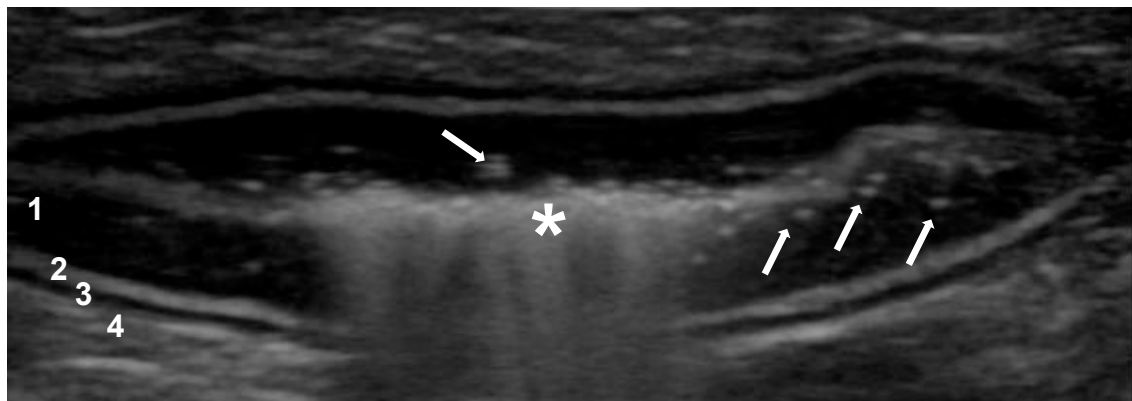


Figure 9 – Mucosal hyperechoic speckles. Note the multiple hyperechoic foci (white arrows) disseminated through the duodenal mucosa of a dog diagnosed with idiopathic inflammatory bowel disease. The gas-filled intestinal lumen, with ultrasonographic gas reflections, is marked by a white asterisk. (1) Mucosa; (2) submucosa; (3) muscularis propria; (4) serosa (not clearly visible, as an outer hyperechoic thin line).

In one study,⁸ dogs with steroid-responsive intestinal disorders frequently had hyperechoic mucosal speckles that did not resolve after treatment, despite clinical improvement. Speckles are non-specific for differentiating disease category and activity, and are suspected to represent chronic intestinal changes, requiring a longer period of time to resolve.⁸ Although hyperechoic speckles have been found to be a sensitive parameter for the presence of inflammatory intestinal disease, dogs presenting with mucosal speckles usually

have only mild clinical signs, that can be managed with symptomatic treatment without the need of intestinal biopsies, and therefore, potential associated intestinal wall inflammation has not been definitely proven.

Finally, a hyperechoic stripe (Figure 10), seen through the mucosal layer of a small intestinal loop in cross-section as a stripe thicker than the mucosa–lumen interface, or as a thick rounded focus on either side of the ultrasonographic image, has also been reported in dogs and is considered a clinically insignificant ultrasonographic finding.¹¹ This stripe is not affected by the type, shape, or frequency of the transducer and its location with respect to the intestinal loop is actually related to the flat shape of the bowel loop, not to the insonation angle. It tends to disappear when the loop is dilated, and plication of the intestinal wall seems to be a necessary condition for its visualization.¹¹

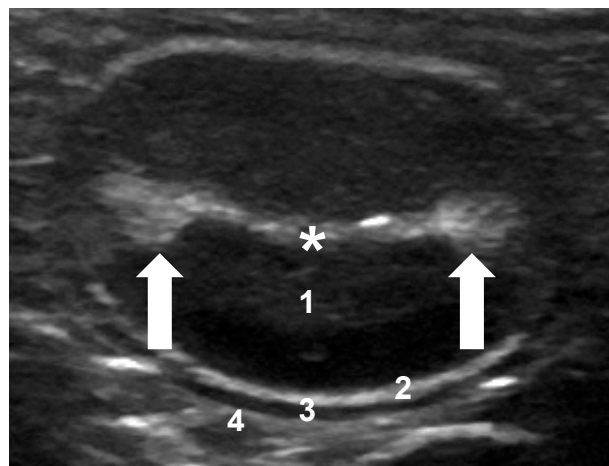


Figure 10 – Hyperechoic mucosal stripe.

Note the round hyperechoic focus in the mucosa at each point of wall flexion on this transverse ultrasonographic image of the jejunal loop of a healthy dog (white arrows). The empty intestinal lumen/lumen-mucosa interface is marked by a white asterisk. (1) Mucosa; (2) submucosa; (3) muscularis propria; (4) serosa.

Histologically, this stripe is located at the point of plication of the intestinal wall, where the mucosal villi appear unevenly displaced, and is therefore suspected to represent an interface in the mucosa where the distance between villi is increased, maybe reinforced by entrapment of mucus or gas bubbles within the intervillous spaces. The hyperechogenicity of this stripe could be due to the mismatch of acoustic impedance between mucosa and mucus, or mucosa and gas.¹¹

I.2.d.iv. Mucosal fibrosis

A thin hyperechoic mucosal band within the mucosa, paralleling the submucosa, has been recently reported in cats. This mucosal feature is different from the hyperechoic mucosal striations or speckles described in dogs.^{8, 10, 11, 60, 62, 63} In 11 cats included in a recent study and diagnosed with segmental mucosal fibrosis using full-thickness intestinal biopsies,⁶³ this hyperechoic mucosal band was observed through several intestinal segments in all cats. Based on ultrasonographic and histopathological comparison, this study concluded that the hyperechoic mucosal band likely represented an ultrasonographic interface due to the presence of mucosal fibrosis described histopathologically.⁶³ Concurrent associated inflammatory cell infiltrate was present histopathologically in all cats, and most of them also had ultrasonographic evidence of intestinal wall thickening and altered intestinal layering.⁶³

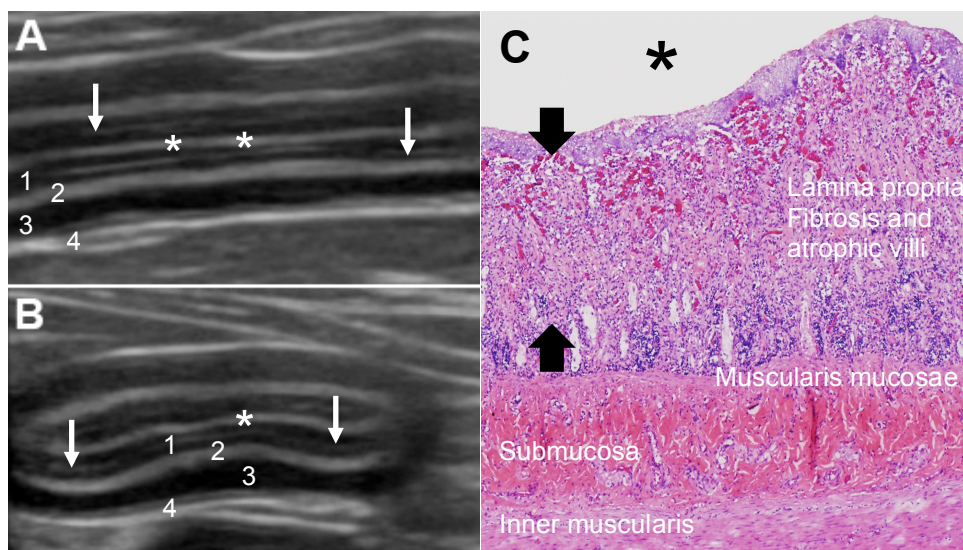


Figure 11 – Mucosal fibrosis in cats.

(A) Longitudinal and (B) transverse images of a jejunal segment of a cat with a thin hyperechoic linear mucosal band paralleling the submucosa (thin white arrows). Mild muscularis layer thickening is also visible. (C) Magnified histological image of the intestinal wall of a small intestine of a 6-month-old cat (different cat than cat of images (A) and (B)) with feline panleukopenia. The lamina propria is diffusely replaced by fibrous connective tissue (fibrosis, between the black arrows) with moderate lymphoplasmacytic infiltration and loss of crypts. Remaining crypts are dilated with loss of epithelium or lined by attenuated epithelium. Villi are blunted, fused, and severely atrophic. The mucosal surface is covered with abundant fibrin (Hematoxylin & Eosin. 100x). The intestinal lumen is marked by asterisks. (1) Mucosa; (2) submucosa; (3) mildly thickened muscularis propria; (4) serosa.

Mucosal fibrosis has been reported with inflammatory bowel disease in cats, with intestinal strictures reported as a potential complication in the most severe cases.⁶⁴⁻⁶⁶ It is

however non-specific, and associated with a variety of inflammatory, neoplastic, and degenerative diseases in a wide variety of tissues.⁶³ It is believed to represent the end result of mucosal inflammation or a response to the secretion of pro-inflammatory cytokines produced in the diseased intestine.^{62, 63, 66, 67} Initially, the mucosal hyperechoic band associated with mucosal fibrosis has been noted in cats in association with other small intestinal changes, such as a thickened muscularis layer, increased echogenicity of the mucosa, or a prominent sub-mucosa.⁶³ However, this hyperechoic mucosal band has also been observed in cats without other ultrasonographic intestinal changes, and without clinical signs related to the digestive system.⁶³ Anecdotally, this hyperechoic mucosal line is also commonly observed in healthy feline patients, without associated inflammatory wall disease. This is further supported by a recent study reporting four cats with full-thickness intestinal biopsies with marked band-shaped intestinal fibrosis of their mucosal lamina propria on histology, without increased inflammatory infiltrate or other architectural changes associated.⁶² Intestinal mucosal fibrosis is also different from feline gastrointestinal eosinophilic sclerosing fibroplasia, where a mass-like intestinal wall lesion, with complete loss of intestinal layering and associated infiltrative mural eosinophilic inflammation, has been reported.⁶⁸ Therefore, visualization of this hyperechoic mucosal band in cats without reported gastrointestinal signs is not considered a reliable feature of active enteropathy, even though it does not exclude the possibility of a previous or clinically silent chronic enteropathy. This line may be an incidental finding in most cats and only now being visualized and reported due to improved resolution of the ultrasonographic transducers.

I.2.d.v. The parallel hyperechoic mucosal line in dogs

In a recent study in dogs,⁶⁰ ultrasonographic mucosal changes have been reported after oral administration of corn oil. In that study, corn oil ingestion resulted in a subjective increase in mucosal echogenicity of at least one segment of small intestine (duodenum, jejunum, or ileum) in 4/5 healthy dogs and 9/9 dogs with lymphangiectasia. This effect was observed as early as 30 minutes after ingestion and persisted up to 120 minutes. Corn oil ingestion increased the conspicuity of ultrasound lesions in dogs with lymphangiectasia, with

the lesions best detected 60 or 90 minutes after the administration of corn oil. In addition, the presence of a transient hyperechoic parallel line within the mucosa of the duodenum and jejunum in 4/5 healthy dogs after corn oil administration (Figure 12) was attributed to an increased visibility of the lymphatic vessels, responsible for uptake of fat from the lacteals, more visible when distended, and was not considered a pathologic finding in these dogs.⁶⁰

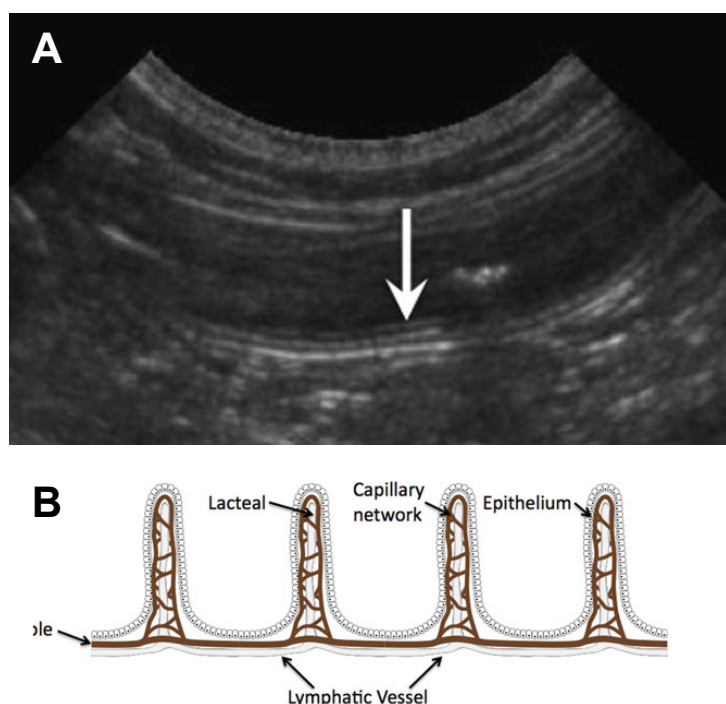


Figure 12 – Parallel hyperechoic mucosal line in dogs. (A) Sagittal image of a jejunal loop of a healthy dog, acquired 30 min after corn oil administration orally. A parallel hyperechoic mucosal line, not visible prior to corn oil administration, is becoming visible within the jejunum (arrow) and is considered to represent a dilated lymphatic vessel, as seen in the schematic (B), illustrating finger-like projections of lacteals within the villi, which connect to the lymphatic vessel for drainage of the small intestine. (From⁶⁰, permission to reuse in Appendix)

In a recent study in healthy dogs,⁶⁹ similar mucosal changes were observed using both low and high fat diets. The dogs included in this study were fasted for a minimum of 12 hours before an abdominal ultrasound was performed. Two high frequency ultrasonographic transducers (a curved and a linear array) were used to examine 3 different jejunal segments and the duodenum. Static small intestinal images were acquired and then reviewed and scored by two radiologists, blinded to diet group and time point, to assign a consensus score for mucosal echogenicity. This study showed that mucosal hyperechogenicities (speckles and striations) were observed at 60 minutes post-prandial for low and high fat diets, and

immediately after ingestion for the high fat diet, and were considered to reflect physiologic lacteal dilation, identified in healthy dogs. According to these studies,^{60, 69} the ultrasonographic mucosal post-prandial appearance described in healthy dogs overlaps the ultrasonographic findings seen in dogs with lymphangiectasia and enteritis, and should therefore be interpreted carefully in dogs that do not present any gastrointestinal clinical signs, as they may merely represent normal mild post-prandial lacteal dilation.

I.2.d.vi. Thickened submucosal intestinal layer

The submucosal layer is the most conspicuous hyperechoic layer of the small intestinal wall. Studies in human medicine have suggested, in correlation with pathologic findings, that increased thickness of the echogenic submucosal layer (Figure 13) indicates an acute disease process, related to either submucosal edema or hemorrhage, while more chronic gastrointestinal diseases, regardless of their cause, appear to lack this prominent echogenic layer, but would rather show effacement of the intestinal layering.⁷⁰

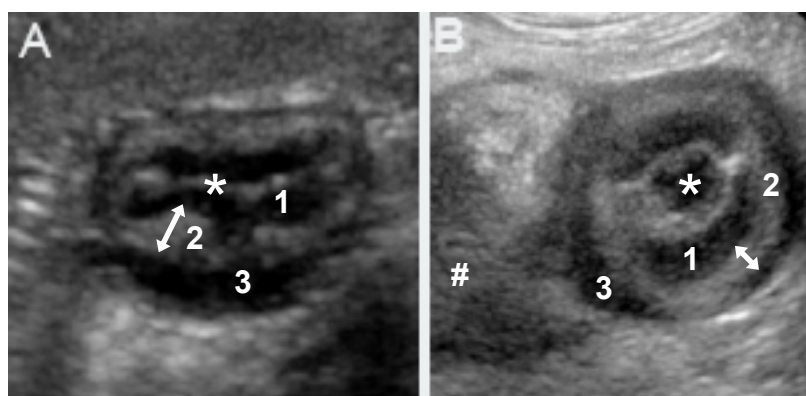


Figure 13 – Duodenal submucosal layer thickening. (A) Transverse ultrasonographic image of a dog diagnosed with *Heterobilharzia* showing irregular thickening of the submucosa (white double arrowhead line). (B) Transverse ultrasonographic image of the duodenum of a dog diagnosed with acute pancreatitis, showing duodenitis, with irregular thickening of the submucosal duodenal layer (white double arrowhead line), increased duodenal wall total thickness and adjacent inflamed right pancreatic limb (white # sign). The intestinal lumen is marked by a white asterisk. (1) Mucosa; (2) submucosa; (3) muscularis propria.

The use of Doppler ultrasonography (color or power Doppler) may be helpful for further differentiation,⁷⁰⁻⁷² as submucosal edema in conjunction with hyperemia of the intestinal wall seen on Doppler evaluation strongly suggests vasodilatation related to an infectious or inflammatory process, while intramural hemorrhage, on the other hand, should

be accompanied by normal to diminished vascularity, with more uniformly hypoechoic intestinal wall thickening, with loss of characteristic layers.⁷¹

In veterinary medicine, small intestinal submucosal layer thickening has been reported with infectious diseases, such as canine schistosomiasis.^{73, 74} In the reported *Heterobilharzia americana* infection cases in dogs, the thickened submucosal layer, which showed evidence of mineralization in some instances, was associated with edema, granulomatous inflammation, and fragmented schistosome eggs.^{73, 74}

I.2.d.vii. Muscularis thickening

Ultrasonographic thickening of the muscularis propria without loss of the intestinal layering (Figure 14) has been reported in cats and associated with diffuse intestinal wall infiltration, either neoplastic (small cell T-cell lymphoma usually, or intestinal mastocytosis less commonly), secondary to inflammatory bowel disease (lymphoplasmacytic or eosinophilic enteritis most commonly), or due to intestinal smooth muscle hypertrophy.^{64, 75-82} Ultrasonographically, a muscularis-to-submucosa ratio >1 in cats is indicative of an abnormal intestinal segment.⁷⁶

In a recent study⁷⁶ comparing the wall layering of cats with inflammatory bowel disease to intestinal lymphoma, there were no ultrasonographic differences found between the two diseases, and the mean thickness of the muscularis propria in cats with intestinal lymphoma or inflammatory bowel disease was similar, measuring twice the thickness of the one of healthy cats, and was the major contributor to significant overall duodenal and jejunal wall thickening. A previous study⁷⁹ found a stronger association between small cell T-cell lymphoma and muscularis layer thickening than with inflammatory bowel disease when considering the prevalence in each population. However, differentiation between the previously mentioned causes of muscularis thickening is not possible ultrasonographically, even though the odds of a cat having lymphoma are higher when muscularis thickening is present.^{62, 64, 75, 76, 78, 79, 83-85} This study, however, was skewed towards cats affected with more severe inflammatory bowel disease, that had full-thickness biopsies, versus more mildly affected cats, which did not receive full thickness biopsies for histological analysis.

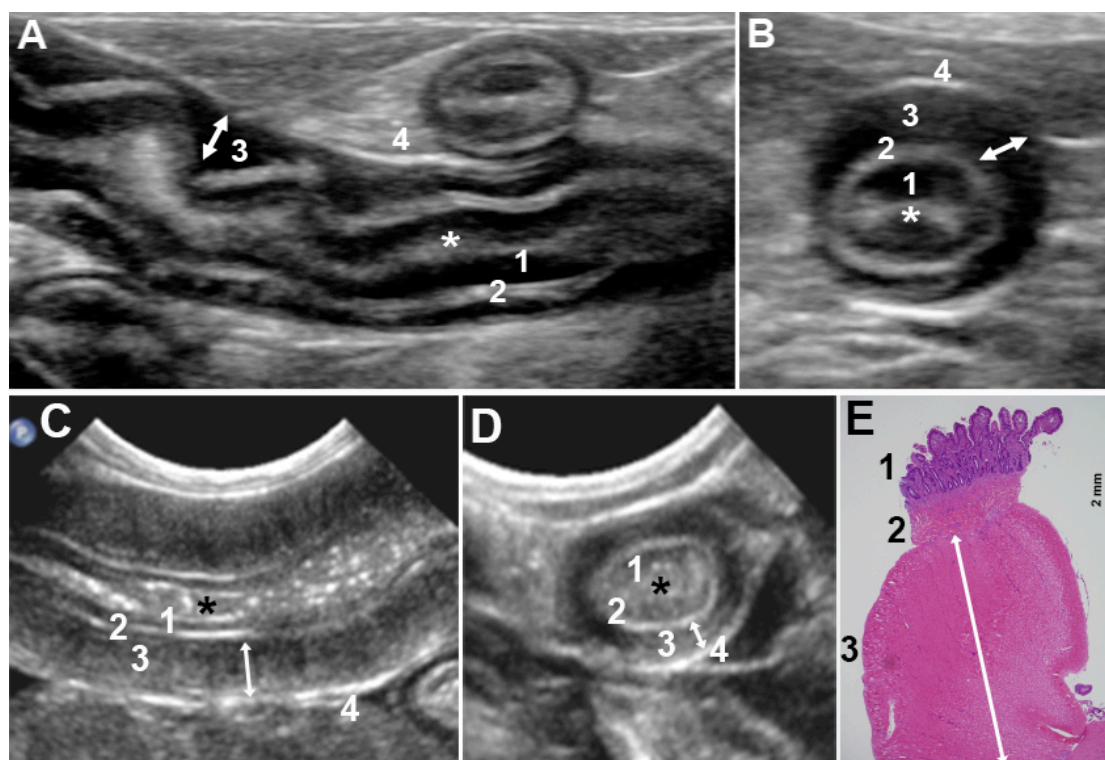


Figure 14 – Muscularis thickening in cats.

(A) Longitudinal and (B) transverse ultrasonographic images of the jejunum of a cat diagnosed with small cell T-cell intestinal lymphoma, showing moderate circumferential diffuse thickening of the muscularis layer (white double arrowhead line) and overall increased thickening of the jejunal wall without loss of intestinal layering. (C) Longitudinal and (D) transverse ultrasonographic images of the jejunum of a cat diagnosed with eosinophilic enteritis, showing severe circumferential diffuse thickening of the muscularis layer (white double arrowhead line), overall increased thickening of the jejunal wall without loss of intestinal layering, and mild diffuse hyperechogenicity of the muscularis layer. (E) Histological image of the intestinal wall of the same cat of images (C) and (D), diagnosed with eosinophilic enteritis, showing severe muscularis hypertrophy (white double arrowhead line) and eosinophilic infiltration (Hematoxylin & Eosin. 10x). The intestinal lumen/lumen-mucosa interface is marked by an asterisk. (1) Mucosa; (2) submucosa; (3) thickened muscularis propria; (4) serosa.

Thickening of the muscularis may be explained by the fact that lymphoma commonly occurs with concurrent lymphoplasmacytic inflammatory bowel disease in cats,^{76, 83, 84, 86} with a chronic inflammatory process suspected to precede, and potentially act as a trigger for, the subsequent onset of gastrointestinal lymphoma,⁸⁷ with a study reporting that up to 60% of the cats involved in that study and diagnosed with lymphoma had prior clinical signs indicative of inflammatory bowel disease.⁸⁸ A possible continuum of disease may therefore explain the similarity of the ultrasonographic appearance of the muscularis propria in both populations of cats with inflammatory bowel disease and small cell lymphoma.

Intestinal smooth muscle hypertrophy has also been described in cats, with the same ultrasonographic pattern than the one reported for lymphoma or inflammatory bowel disease, consisting of a diffuse circumferential muscularis layer thickening without loss of intestinal layering.^{81, 82} A similar condition has been reported in horses and other herbivores, pigs, and humans,^{80, 89-91} and also experimentally reproduced in rats, guinea pigs, and pigs by creating a surgical stenosis of the small intestine.⁹¹⁻⁹³ It can occur either as a compensatory mechanism, for instance in response to distal intestinal stenosis (called in this case secondary hypertrophy) or in the absence of a detectable stenosis (and therefore called idiopathic or primary hypertrophy). Primary muscularis hypertrophy can affect the entire intestine, cause malabsorption, and is often associated with severe chronic enteritis and decreased functional properties.⁸² The association of chronic enteritis with idiopathic muscularis hypertrophy in cats suggests that factors released in intestinal inflammation may also act as hypertrophy stimuli for smooth muscle cells.⁸² In both forms, the hypertrophied muscle can narrow the intestinal lumen and cause obstruction.⁹⁰ The distinction of muscularis hypertrophy with the previously described infiltrative intestinal wall disease (inflammatory bowel disease or neoplasia) is not possible ultrasonographically. Actually in several studies with inflammatory bowel disease or small cell T-cell lymphoma in cats, in which distal intestinal biopsies were performed away from the most severe site of intestinal lesions, muscularis layer enlargement did not demonstrate inflammatory or neoplastic cells infiltrating the muscularis layer, and was therefore considered secondary to muscularis hypertrophy rather than infiltrative neoplastic or inflammatory disease.^{76, 78, 79, 81, 82}

I.3. Histological and Ultrasonographic Intestinal Layering Correlation

As previously described, five to nine intestinal layers can be observed ultrasonographically, depending on the region of the gastrointestinal tract being examined and the frequency and operating characteristics of the ultrasonographic transducer.^{3, 4, 6, 12, 14-16, 42, 94, 95} Initial interpretation of the ultrasonographic images assumed direct correlation between the layers seen on ultrasound and those seen on histology.^{16, 25, 39-41, 96} However,

there was later disagreement in human medicine concerning this correlation.^{24, 97} Ex vivo studies revealed that interface echoes should also be taken into account^{12, 24} and that the ultrasonographic intestinal layers had a slightly different thickness than the histological layers, since they could be either included or covered by interface echoes.

With the five layer ultrasonographic model, when precise measurements of the histological layers were compared with measurements of the layers on ultrasonographic images performed on ex vivo samples, it was shown that the first hyperechoic ultrasonographic layer appeared to be thinner than the true mucosal thickness, and that it actually corresponded to the interface echo between the ultrasound coupling medium and the mucosal surface.¹⁶ Similarly, the third layer on ultrasound images (the ultrasonographic submucosa) was slightly thicker than the corresponding histological submucosa and the fourth layer on ultrasonographic images (the ultrasonographic muscularis layer) was slightly thinner than the histological muscularis propria.^{12, 24} It was therefore concluded that, rather than correlating with the histological layers, the five intestinal layers observed on ultrasound corresponded to the following (Figure 15A and Table 2) histological layers:

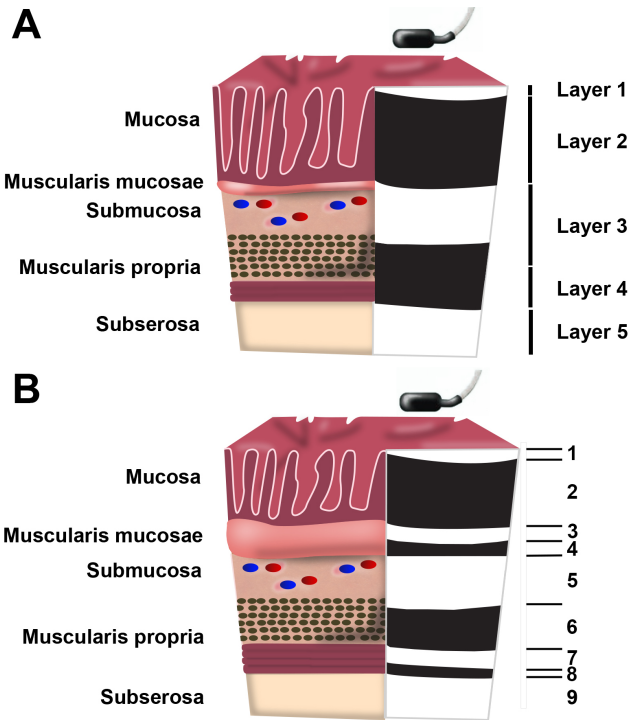


Figure 15 – Relationship between histological and ultrasonographic intestinal wall layers. (A) The ultrasonographic five and (B) nine-layer gastrointestinal wall structure. The numbered layers correspond to the layers of the Table 2 and Table 3, respectively. (Adapted from¹⁵)

Table 2 – The five-layered gastrointestinal wall on ultrasound imaging.

US	Corresponding histological structure
1	superficial mucosa
2	deep mucosa
3	submucosa plus acoustic interface between submucosa and muscularis propria
4	muscularis propria minus acoustic interface between submucosa and muscularis propria
5	serosa and subserosal fat

Similarly, with the development of high-frequency endoscopic ultrasonography, the nine-layer intestinal wall model was described, and when compared to histology,¹² these nine layers corresponded to the following (Table 3 and Figure 15):

Table 3 – The nine-layered gastrointestinal wall on EUS imaging.

US	Corresponding histological structure
1	Epithelial interface
2	Epithelium
3	Lamina propria plus acoustic interface between lamina propria and muscularis mucosa
4	Muscularis mucosa minus acoustic interface between lamina propria and muscularis mucosa
5	Submucosa plus acoustic interface between submucosa and inner muscularis propria
6	Inner muscularis propria minus interface between submucosa and inner muscularis propria
7	Fibrous tissue band separating inner and outer muscularis propria
8	Outer muscularis propria
9	Serosa and serosal fat

These discrepancies between the intestinal layers observed on histology and ultrasound may be explained by ultrasonographic basic physical concepts. In ultrasound imaging, discrimination between two distinct points depends on the spatial resolution of the ultrasound beam. The axial resolution is the ability to discriminate between two distinct points along the axis of the ultrasound beam, and is probably the most important factor allowing visualization of the different intestinal layers. It is usually limited by the spatial pulse length (SPL) of the ultrasonographic beam, which is determined by the following equation:^{16, 33, 35}

$$SPL = \frac{c}{f} \cdot n$$

where c is the speed of sound in tissue (1540 m.s^{-1}), f is the frequency of the transducer, and n is the number of cycles per pulse. The term c/f is also equivalent to the wavelength (λ) of the ultrasound pulse in the tissue.^{33, 35} The limit of axial resolution is equal to half the spatial

pulse length, and therefore, if for instance we take an ideal ultrasonographic transducer, emitting a pulse of one cycle in duration, if the frequency of this pulse is 10 MHz, then the spatial pulse length will be approximately 0.15 mm. Thus, at best, this ideal transducer will only be able to resolve two structures that are separated by a distance greater than 0.075 mm. If the distance between these two structures is less than this value, they will then be observed as a single structure on the ultrasonographic image.¹¹ Furthermore, all reflective interfaces will have a thickness equal to that of the spatial pulse length (Figure 16). In reality, the spatial pulse length is governed by the frequency and damping of the transducer. Higher frequencies and rapid damping transducers will have a shorter spatial pulse length resulting in better axial resolution.^{16, 33, 35} Axial resolution is the most important property in imaging the layered structures of the gastrointestinal tract wall.¹¹

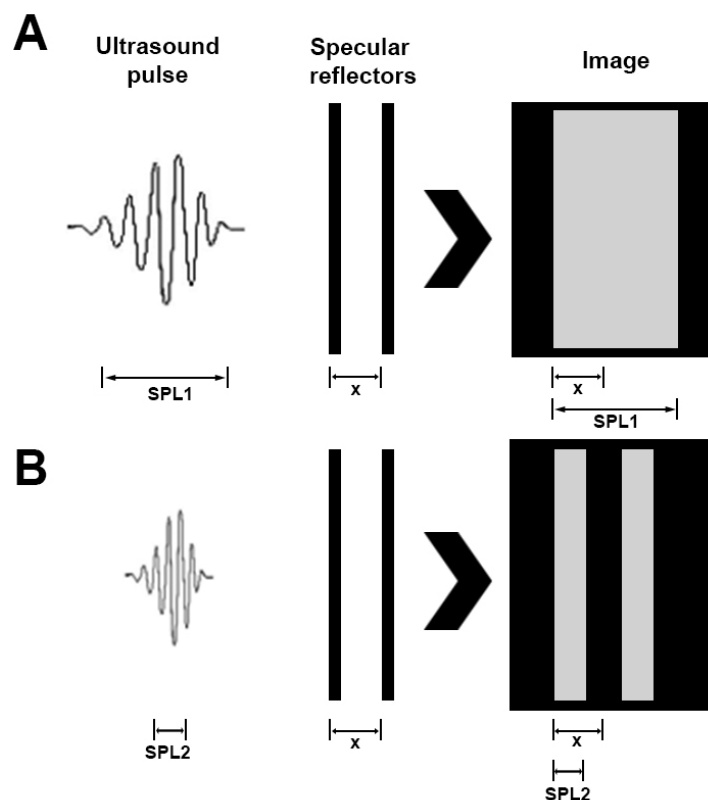


Figure 16 – Principle of ultrasonographic axial resolution.

A pulse generated by an ultrasound transducer has a spatial pulse length (SPL) determined by the frequency, number of cycles, and the sound velocity in the propagating tissue. A lower frequency pulse (A), with a long SPL (greater than twice the distance between the two specular reflectors), will be unable to resolve the two different reflectors and the resulting image will be a single reflector with an axial depth equal to the SPL. On the contrary, a higher frequency pulse (B), with a short SPL, less than twice the distance between the two specular reflectors, will be able to resolve the two separate reflectors and the depth of each reflector on the ultrasound image will be equal to the SPL of the ultrasound pulse. (Adapted from¹⁶)

As previously mentioned, on ultrasonographic images, it was found that the hyperechoic third intestinal layer was slightly thicker than the corresponding histological submucosa, and that the fourth hypoechoic intestinal layer on ultrasound was slightly thinner than the histological muscularis propria.¹⁵ Based on the physical principle previously explained, this is considered most likely due to the interface echo band created from the boundary between the submucosa and the muscularis propria, which adds thickness to the submucosal layer on the ultrasonographic images, and detracts from the thickness of the muscularis propria layer. The thickness of this interface echo is related to the axial resolution of the US transducer, which is only approximately 300 μm with the current high-frequency transducers used in endoscopic ultrasound machines.²⁴ Similarly, the muscularis mucosae also adds thickness to the third US layer, as the normal muscularis mucosae is thinner than the interface echoes, and therefore is obscured by this interface echo between the lamina propria and the muscularis mucosae, which then blends with the echoes from the underlying submucosa.¹³

Additional discrepancies in tissue layer thickness between histological and endoscopic ultrasound images were also attributed to shrinkage of tissue during histological processing and possibly variations in acoustic propagation velocities in the different tissue layers.²⁴ It was also reported that compression of the intestinal wall could cause a reduction in both the wall thickness and the number of layers.⁹⁸ However, these small discrepancies from histology appear to be minimal and have not yet been proven to be clinically important in the interpretation of intestinal endoscopic ultrasonographic images.^{15, 16, 24}

CHAPTER II – CORRELATION OF ULTRASONOGRAPHIC SMALL INTESTINAL WALL LAYERING WITH HISTOLOGY IN NORMAL DOGS

II.1. Materials and Methods

Twelve dogs, euthanized for reasons unrelated to gastrointestinal disease, were included in the study: 6 intact males and 6 intact females. Seven of them were mixed breed dogs, and 5 were Pitbull-type dogs. All were mid-sized dogs, with an average weight of 23.4 ± 5.2 kg (10 dogs between 15-30kg and 2 dogs between 30-35kg), and originating from the same animal shelter. Extensive medical history was not available. Age was not precisely known, but the dogs were all assumed to be young adults, based on dentition and physical appearance.

II.1.a. Ultrasonographic and histological image acquisition

The small intestinal samples were resected immediately (no longer than 1h) after humane euthanasia, and consisted of 3-4 cm in length segments of the mid-duodenum, mid-jejunum, and mid-ileum. After resection, each sample was individually pinned, using 22 G needles (to avoid shrinkage of the sample between euthanasia and histological processing), on a Petri dish containing a thick layer of paraffin acting as a support for the pinning needles, and an additional layer of agar added over the paraffin to serve as a hypoechoic layer, to allow better visualization of the outer intestinal wall margins during the ultrasonographic examination. The Petri dish was then placed in a water-filled container, and transverse B-mode ultrasonographic images were acquired using a portable ultrasonographic machine, with a linear 13 MHz transducer¹ (Figure 17). The footprint of the transducer was placed in a similar position for each sample and was not in direct contact with the intestinal surface, to avoid applying pressure on the intestinal sample. The ultrasound focus was set at the level of the intestinal lumen. Using ultrasonographic guidance, two 22 G needles were then placed at an approximate 45-degree angle on each side of the intestinal loops, without penetrating the intestinal wall, to mark the site where the images were obtained, so that the histological transverse sections could be taken at the same level, for adequate comparison (Figure 17B).

¹ Logiq e vet, 12L-RS electronic linear transducer, GE Healthcare, Little Chalfont, UK.

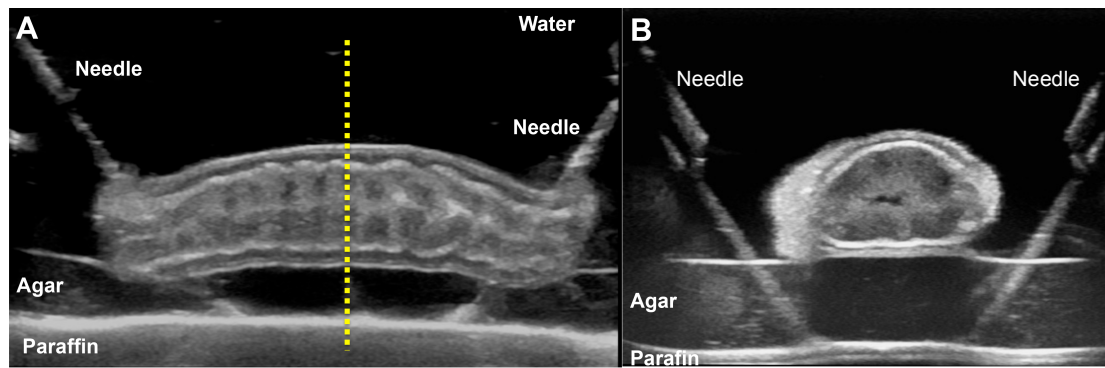


Figure 17 – Small intestinal loops ultrasonographic images acquisition. (A) Longitudinal image of a jejunal sample pinned on a layer of paraffin and a layer of agar, and immersed in a water bath. (B) Transverse ultrasonographic image acquired at the level of the vertical dotted line on the image (A). Two needles are visible on each side of the intestinal sample to mark the area where the ultrasonographic measurements were performed.

After acquisition of the ultrasonographic images, each Petri dish (with the pinned intestinal samples) was placed in a 10% buffered formalin-filled individual container. Due to the delay between the ultrasonographic imaging acquisition and the histological processing of the samples (approximately 5 days) and because the intestinal samples were placed in formalin, shrinkage of the intestinal samples was of concern when attempts for measurement of intestinal layer thickness comparisons were considered.⁹⁹ Therefore ultrasonographic images were repeated 48 to 72h post- formalin fixation, to rule out any difference between the two sets of ultrasonographic measurements pre- and post-formalin and allow adequate comparison with the histological images. The same linear 13 MHz transducer¹, and a second linear transducer², of higher resolution (15 MHz), were used post-formalin fixation to acquire ultrasonographic images at the same level than the one obtained immediately post-mortem.

After formalin tissue fixation, the intestinal samples were then processed routinely, embedded in paraffin, sectioned in 1.5-5 mm thick slices (depending on the intestinal sample size, with the duodenum having the thickest slices) and stained with hematoxylin and eosin, with the histological section performed at the level of the needles pinned on each sides of the intestinal loops, marking the emplacement where the transverse ultrasonographic images had been acquired (Figure 17B). The histological sections were then digitally scanned for later histological evaluation³.

¹ Logiq e vet, 12L-RS electronic linear transducer, GE Healthcare, Little Chalfont, UK.

² Logiq S8, ML6 electronic linear transducer, GE Healthcare, Little Chalfont, UK.

³ NanoZoomer-XR, Hamamatsu NanoZoomer system, Bridgewater, NJ 08807, U.S.A.

II.1.b. Ultrasonographic and histological images review and mensuration

The ultrasonographic images were saved in a DICOM format and were analyzed by the same operator, using the same post-processing image viewer application⁴. Measurements were randomly performed 3 times by the same operator and consisted of a total of 7 measures (Figure 18): the total intestinal ultrasonographic thickness, the mucosal ultrasonographic thickness, the submucosal ultrasonographic thickness, the muscularis ultrasonographic thickness (an inner and outer part were observed and therefore both were measured in addition to the total muscularis ultrasonographic thickness), and the serosal ultrasonographic thickness.

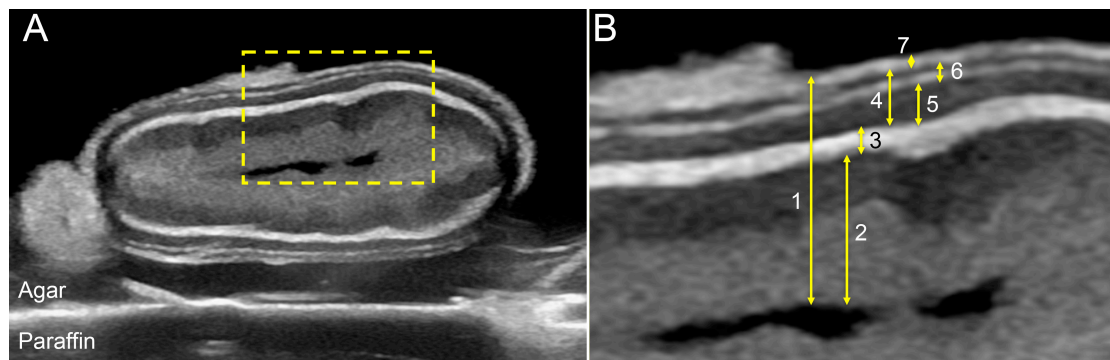


Figure 18 – Ultrasonographic measurements of the different small intestinal layers. (A) Transverse image of the jejunum of a dog, and magnified (dotted rectangle on (A)) ultrasonographic image (B) of the intestinal wall, showing the different measurements performed on the ultrasonographic images. (1) Total thickness; (2) Mucosa; (3) Submucosa; (4) Muscularis propria layer; (5) Inner layer of the muscularis propria; (6) Outer layer of the muscularis propria; (7) Serosa.

Intestinal histological layer thickness measurements were similarly performed by the same operator, using the same whole slide image viewer software⁵; the measurements were performed randomly and repeated 3 times. They consisted of the total intestinal histological thickness, the mucosal histological thickness, the submucosal histological thickness, the inner muscularis histological thickness, the outer muscularis histological thickness, the total muscularis histological thickness, and the serosal histological thickness (Figure 2).

II.1.c. Statistical assessment

Measurements of total wall thickness, mucosa, submucosa, muscularis (inner layer, outer layer, and total muscularis thickness) and serosa were compared between the

⁴ OsiriX Imaging Software, Ayca Digitalssysteme GmbH, Wuerzburg, Germany.

⁵ NDP.View 1.1.4, Hamamatsu NanoZoomer system, Bridgewater, NJ 08807, U.S.A.

ultrasonographic and histological results. A statistical software⁶ was used to analyze the data as an analysis of variance of a mixed effects model. Fixed effects in the model included Organ (jejunum, duodenum, or ileum), Method (ultrasound or histology), Parameter (the different intestinal layers measured) and the two- and three-way interactions of these effects. The random effect was Dog. When overall significant differences were found, post-hoc pairwise comparisons were conducted with t-tests of least-squares means for main effects and for interaction effects. All comparisons were considered significant at $p < 0.05$.

II.1.d. Subjective assessment

Subjective evaluation of the histological and ultrasonographic images was also performed. Histological evaluation of each intestinal sample was achieved by a board-certified pathologist, assessing the quality of the histological samples, as well as possible cellular infiltration or presence of histological abnormalities within the intestinal samples. On the ultrasonographic images, the overall wall layering was assessed by a board-certified radiologist, and the presence of additional layers was reviewed, along with the evaluation of the different layer echogenicity and layer thicknesses. Finally, simultaneous comparison between the ultrasonographic images and histological samples was performed by both the radiologist and pathologist to try to correlate potential ultrasonographic additional layers or changes of intestinal layer echogenicity with histological changes.

II.2. Results

Thirty-six intestinal samples (12 duodenal, 12 jejunal and 12 ileal intestinal samples) were available for interpretation. Four of the 36 intestinal samples required re-cutting for histological analysis, as the sliced samples were of low quality, precluding adequate comparison with the ultrasonographic images (Figure 19 and Figure 20).

The jejunal and ileal samples of one of the dogs were excluded because the samples were thought to have been erroneously switched between the ultrasonographic measurements and histological processing (jejunum thought to be labeled ileum and vice versa).

⁶ SAS® MIXED procedure, SAS Institute Inc., Cary, NC 27513, USA

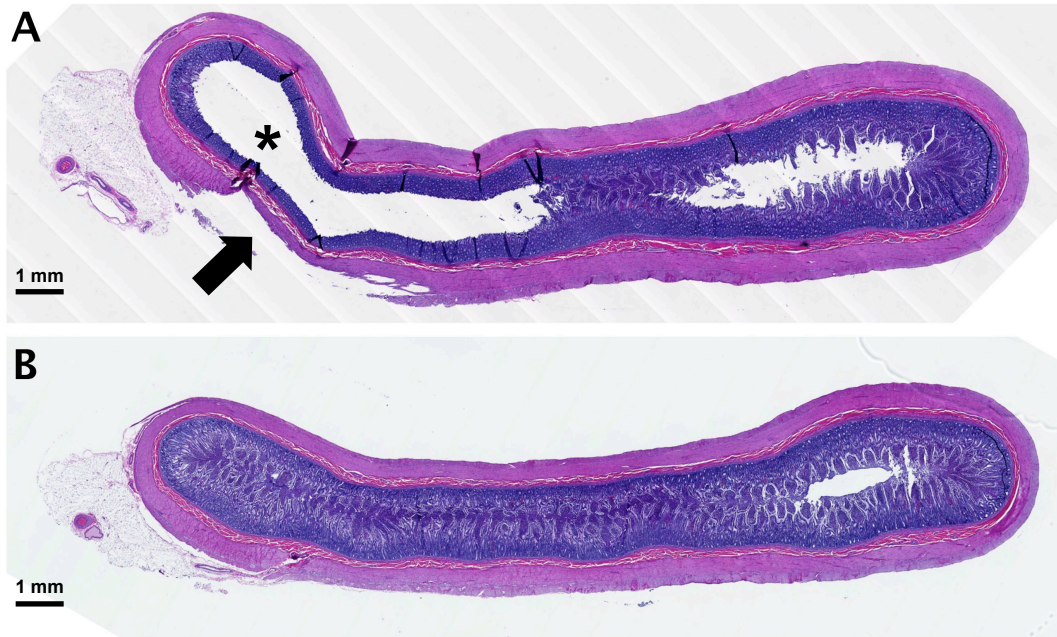


Figure 19 – Jejunal altered histological sample.
Prior to recut (A), most of the epithelium is missing (black asterisk), as well as part of the muscularis propria and serosa (black arrow), and the sample has been crushed during sectioning. The image (B) is a recut section of the same jejunal sample than image (A).

Some of the intestinal samples also demonstrated mild submucosal detachment (Figure 20B), and when the histological measurements were performed, avoidance of these areas was attempted, to try to prevent over-measurement of this layer ultrasonographically.

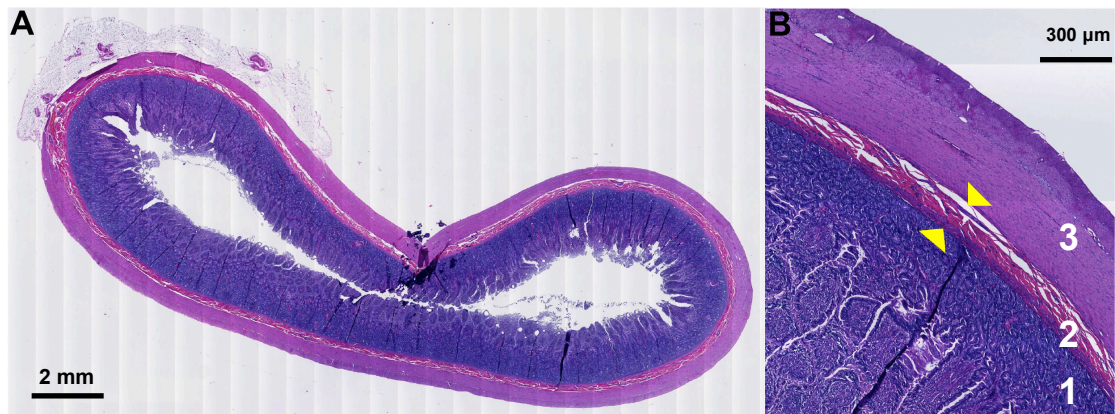


Figure 20 – Crushed histological duodenal sample and mild submucosal layer detachment.
On image (A), the duodenal wall was crushed after histological section. On the magnified image (B) of the intestinal wall, mild submucosal detachment (between the yellow arrowheads) can be seen, with a mild spacing between the muscularis propria and submucosa. (1) Mucosal lamina propria; (2) submucosa; (3) muscularis propria layer.

One of the duodenal samples had multifocal inflammatory infiltration in the mucosal lamina propria, with a mixture of eosinophils and lymphocytes, fewer macrophages and plasma cells, as well as probable mast cells. In the same sample, a focal aggregate of

probable mast cells in the submucosa, possibly in lymphatic, was also observed. The ultrasonographic images of this dog did not reveal any ultrasonographic changes suggestive of an infiltrative intestinal wall disease and therefore it was not excluded from the study.

The small intestinal samples of 2 dogs contained microfilariae (Figure 21), and all the intestinal samples contained a mild-to-moderate increase in eosinophils in their mucosal lamina propria, which is considered a common finding in animals, including clinically healthy dogs in our population.

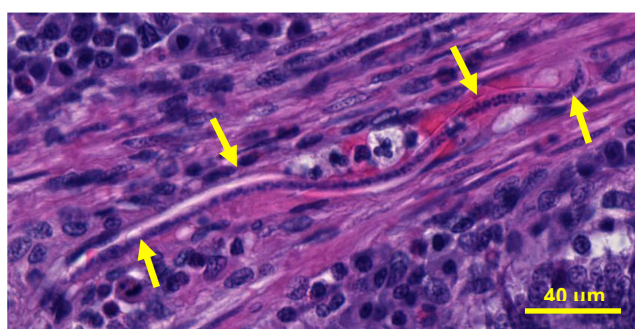


Figure 21 – Mucosal microfilaria in a dog. Magnified histological image showing a microfilaria in the mucosal lamina propria of a jejunal sample in one of our dogs (yellow arrows).

II.2.a. Subjective assessment

In all intestinal samples, the ultrasonographic mucosal layer had a dual echogenicity, with the inner part of the mucosa (closer to the intestinal lumen) being more echoic than its outer part (Figure 22). When compared with the histological samples, the inner part of the mucosa on the ultrasound images, which appeared more hyperechoic than the rest of the mucosa, was consistent with the epithelium/intestinal villi on histology, while the outer mucosal area, more hypoechoic, corresponded to the lamina propria (+/- the muscularis mucosa) histologically. In addition, the degree of hyperechogenicity of the inner portion of the mucosal layer varied among samples (Figure 23). Six of the duodenal samples, and 1 of the jejunal samples had a subjectively severe hyperechoic inner mucosa (Figure 23D). When compared with histology, all of these samples but one (one of the duodenal samples) had mild-to-moderate lacteal dilation observed within the intestinal villi on histology (Figure 23E and Figure 23F), while the samples without this inner hyperechogenicity did not show any histological evidence of lacteal dilation (Figure 23B and Figure 23C).

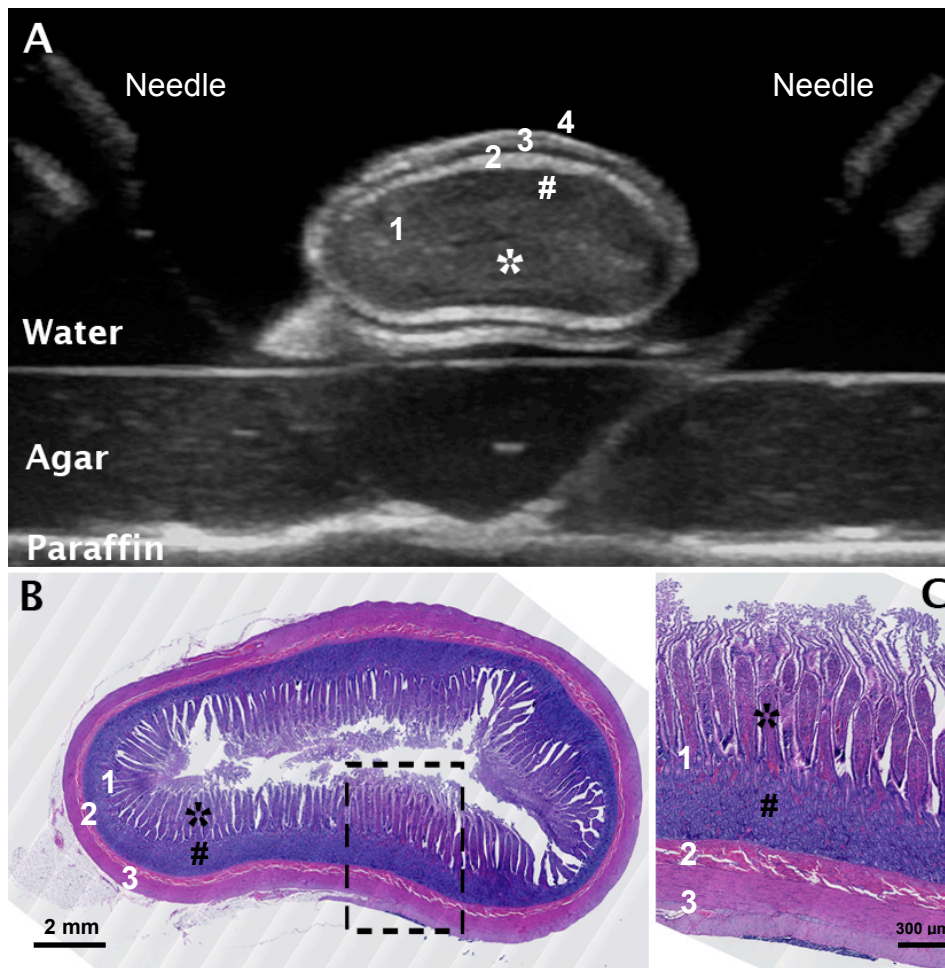


Figure 22 - Ultrasonographic small intestinal mucosal layer dual echogenicity.

(A) Transverse image of the jejunum of a dog, after pinning of the intestinal sample on the Petri dish and immersion in a water bath. Note the two needles on each side of the sample, used to denote the site where the ultrasonographic images were performed, for later processing. (B) Histological transverse section (hematoxylin and eosin stain) performed at the same level as the ultrasonographic image (A). The image (C) (hematoxylin and eosin stain) represents a magnified view (dotted black rectangle on image (B)) of the jejunal wall. In these 3 images, the asterisk (*) marks the localization of the intestinal epithelium, which appears faintly more hyperechoic than the rest of the mucosal layer (lamina propria and muscularis mucosae, # sign) on the ultrasonographic image. (1) Mucosa; (2) submucosa; (3) muscularis propria; (4) serosa.

On the subjective evaluation of the ultrasonographic images, an additional thin hyperechoic line was observed in the muscularis layer of all small intestinal samples. This hyperechoic line was in a similar position in all samples, at approximately the outer second one-third of the ultrasonographic muscularis layer (Figure 24). When reviewed in association with the histological samples, this thin additional ultrasonographic line was considered likely caused by a normal minimal amount of fibrous tissue present between the inner circular and outer longitudinal components of the muscularis propria, and/or due to an interface echo artifact between these two muscle layers.

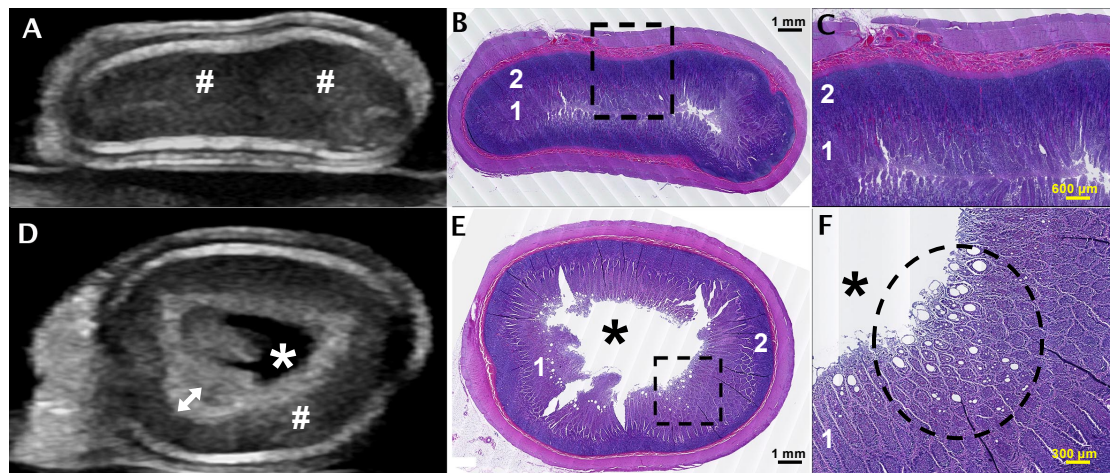


Figure 23 – Degree of ultrasonographic small intestinal mucosal layer dual echogenicity depending on lacteal dilation.

Transverse ultrasonographic ((A) and (D)) and histological ((B), (C), (E), and (F), hematoxylin and eosin stain) images of the duodenal (A) and jejunal (B) sample of two different dogs. The images (B) and (E) have been performed at the same level than the ultrasonographic images (A) and (D) respectively, and the images (C) and (F) correspond to a magnified view of the histological samples (dotted black squares on (C) and (E)). On image (A), a faintly hyperechoic area (white # signs) can be observed in the most inner part of the mucosa, corresponding to the epithelium (1) on the histological images. There is no evidence of lacteal dilation observed on histology in this sample. On image (D), the most inner aspect of the mucosa is severely hyperechoic, and surrounded by a more faintly echoic area within the mucosa (white # sign, likely representing the epithelium). In this sample, mild-to-moderate dilation of the lacteals was noted in the inner aspect of the mucosal epithelium (as seen on (E) and (F) images, dotted circle line), and was assumed to be the cause of the severe hyperechogenicity observed in the inner part of the mucosa on the ultrasound image. The asterisk represents the dilated intestinal lumen. (1) Mucosal epithelium; (2) mucosal lamina propria.

Four of the ileal samples also showed an additional hyperechoic thin line parallel to the submucosal layer on the ultrasonographic images, in the most outer part of the mucosal layer. Histologically, the main difference between these 4 samples and the other ileal samples was the presence of enlarged submucosal lymphoid follicle (Peyer's patch) extending into the lamina propria (Figure 25D-E). The localization of this thin hyperechoic line was in the same location as the histological interface between the enlarged submucosal lymphoid follicles and the lamina propria. In the intestinal samples where this line was not observed, there was no evidence of enlarged submucosal lymphoid follicle noted histologically (Figure 25A-C).

Finally, when subjectively comparing the thickness of the serosal ultrasonographic layer with the real thickness of the serosa on histology (on the histological and ultrasonographic images and when comparing the mean values of the measurements, summarized in Table 4 and Table 5), it appeared that the ultrasonographic layer considered to represent the serosa on ultrasound was much thicker compared to the histological serosal

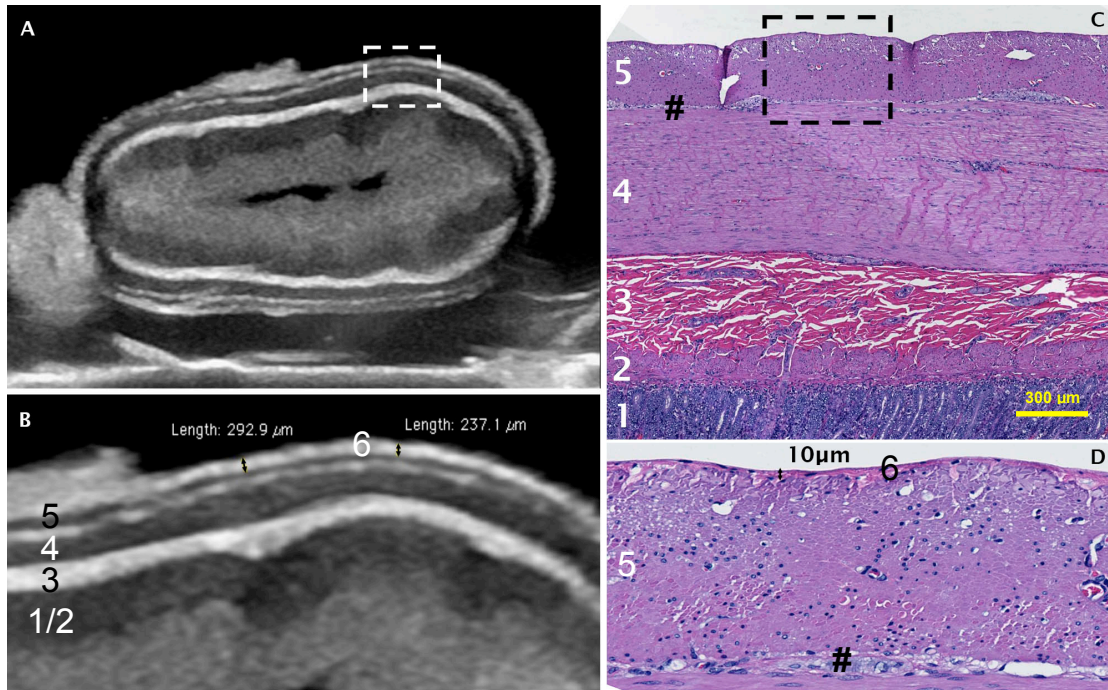


Figure 24 – The hyperechoic muscularis layer interface.

(A) Transverse ultrasonographic image of the jejunum of a dog, and magnified (dotted white rectangle on (A)) (B) image of the intestinal wall (B), showing a hyperechoic thin muscularis line. The histological section (C) (hematoxylin and eosin stain) was performed at the same level than image (A) and is a magnified area of the dotted white rectangle on (A). Note the intestinal layers: (1) mucosal lamina propria; (2) muscularis mucosae; (3) submucosa; (4) inner circular muscularis and (5) outer longitudinal muscularis; (6) serosa. A faint amount of fibrous tissue can be seen between the two parts of the muscularis layer (images (C) and (D), black # sign). The serosa (6) on the image (C) is too thin to be visualized. It can barely be seen on the image (D) (hematoxylin and eosin stain), which is a magnified view of the outer jejunal wall (dotted black rectangle of image (C)). Note the difference in thickness subjectively and quantitatively between the measured ultrasonographic and histological serosal layers (6) on images (B) and (D) respectively.

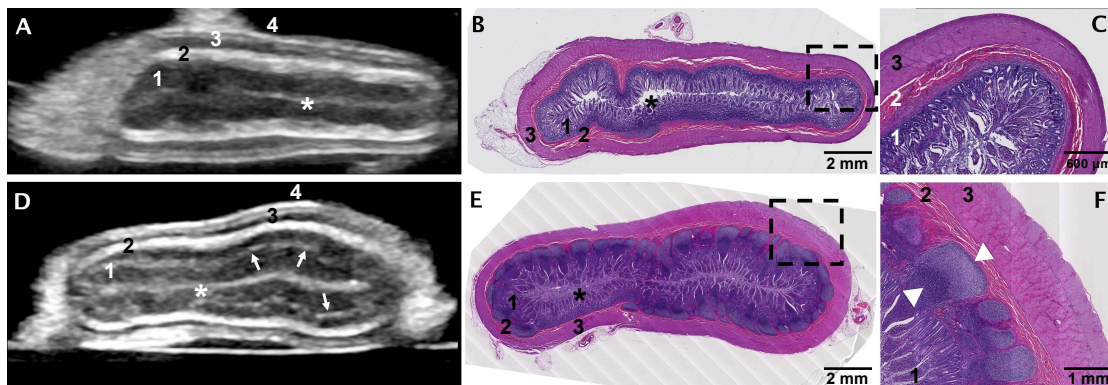


Figure 25 – Ileal echogenic mucosal line and its correlation with enlarged Peyer's patches.

Transverse ultrasonographic images ((A) and (D)) of the ileum of 2 dogs and their relative histological sections ((B) and (E), hematoxylin and eosin stain). (C) and (F) are magnified histological sections from the dotted black rectangle of image (B) and (E) respectively. Note the additional thin hyperechoic interface/layer observed within the mucosa on (D) (white arrows). The main histologic difference between the 2 dogs was the presence of enlarged submucosal lymphoid follicles (Peyer's patches) extending into the lamina propria (image (F), white arrowheads) in the dog with the additional hyperechoic mucosal line. The asterisks mark the intestinal lumen. (1) Mucosa; (2) submucosa; (3) muscularis propria; (4) serosa.

layer which is composed of a single layer of mesothelial cells, with a 6 to 12 times difference noted between both measurements (Figure 24B, Figure 24D, Table 4 and Table 5).

Table 4 – Mean \pm standard deviation (SD) and range values for thickness of the duodenal, jejunal and ileal wall layers measured ultrasonographically.

Layer	Duodenum (n = 12)		Jejunum (n = 11)		Ileum (n = 11)	
	Mean \pm SD (mm)	Range (mm)	Mean \pm SD (mm)	Range (mm)	Mean \pm SD (mm)	Range (mm)
Mucosa	3.58 \pm 0.78	1.82-4.75	2.74 \pm 0.8	0.81-4.11	2.84 \pm 0.94	1.31-4.58
Submucosa	0.41 \pm 0.06	0.31-0.52	0.32 \pm 0.09	0.21-0.57	0.33 \pm 0.1	0.23-0.69
Muscularis	1.08 \pm 0.32	0.57-1.68	0.95 \pm 0.63	0.49-2.88	1.13 \pm 0.63	0.12-2.71
Muscularis inner layer	0.73 \pm 0.25	0.36-1.17	0.65 \pm 0.45	0.32-1.99	0.83 \pm 0.48	0.36-2.15
Muscularis outer layer	0.33 \pm 0.1	0.19-0.54	0.29 \pm 0.17	0.15-0.84	0.35 \pm 0.11	0.2-0.56
Serosa	0.19 \pm 0.06	0.1-0.33	0.16 \pm 0.05	0.09-0.25	0.19 \pm 0.06	0.07-0.33
Total thickness	5.57 \pm 1.02	3.16-6.85	4.46 \pm 1.17	1.97-7.01	4.83 \pm 1.22	2.51-7.18

Table 5 – Mean \pm standard deviation (SD) and range values for thickness of the duodenal, jejunal and ileal wall layers measured histologically.

Layer	Duodenum (n = 12)		Jejunum (n = 11)		Ileum (n = 11)	
	Mean \pm SD (mm)	Range (mm)	Mean \pm SD (mm)	Range (mm)	Mean \pm SD (mm)	Range (mm)
Mucosa	3.54 \pm 0.74	1.97-4.83	2.71 \pm 0.91	1.2-4.25	2.74 \pm 0.92	1.25-4.4
Submucosa	0.26 \pm 0.08	0.09-0.45	0.18 \pm 0.07	0.06-0.36	0.2 \pm 0.09	0.09-0.45
Muscularis	1.04 \pm 0.35	0.5-1.73	0.96 \pm 0.63	0.46-2.84	1.23 \pm 0.6	0.65-2.91
Muscularis inner layer	0.67 \pm 0.23	0.32-1.09	0.61 \pm 0.43	0.03-1.93	0.87 \pm 0.46	0.45-2.18
Muscularis outer layer	0.37 \pm 0.14	0.16-0.65	0.33 \pm 0.21	0.09-0.97	0.36 \pm 0.16	0.13-0.74
Serosa	0.02 \pm 0.01	0.01-0.04	0.02 \pm 0.01	0.01-0.05	0.03 \pm 0.01	0.01-0.05
Total thickness	4.91 \pm 1.03	2.78-6.49	3.92 \pm 1.25	1.94-6.67	4.14 \pm 0.97	2.32-5.5

II.2.b. Statistical assessment

The total thickness of each intestinal segment (duodenum, jejunum and ileum) did not show any statistical significance pre- and post-formalin. This was denoted by the Organ*Method interaction, where no statistically significant difference was seen ($p=0.5756$). There was also no statistical difference noted for any of the intestinal layer thicknesses between ultrasound and histology, for the 3 intestinal segments (duodenum,

jejunum and ileum). This was denoted by the Organ*Method*Parameter interaction, where no statistically significant difference was seen ($p=0.9001$).

II.3. Discussion

Results demonstrated that the ultrasonographic and histological intestinal layers thicknesses correlated, and that additional intestinal layers/ultrasonographic interfaces can be observed in the normal canine small intestine, contrary to what has been previously reported in people.^{12, 16, 24, 97} These additional lines represent normal interfaces between existing histological intestinal layers, such as the thin hyperechoic interface line observed between the inner and outer part of the muscularis propria, or histopathological findings, such as lymphoid follicle hyperplasia, which was likely observed as a thin hyperechoic line in 4 of our ileal samples. Despite the ex vivo characteristic of this study, similar ultrasonographic findings have been observed by the authors during clinical work (Figure 26).

Some of the findings in this study are in accordance with the human literature, where the five ultrasonographic layer model has been questioned and additional layers described as well.^{12, 14, 24} In fact currently, when using endoscopic high-frequency ultrasound, it is possible to distinguish up to nine intestinal layers/interfaces:^{12, 14-16, 39} the luminal/epithelial interface, the epithelium, the lamina propria plus acoustic interface between lamina propria and muscularis mucosa, the muscularis mucosae minus acoustic interface between lamina propria and muscularis mucosa, the submucosa plus acoustic interface between submucosa and inner muscularis propria, the inner muscularis propria minus interface between submucosa and inner muscularis propria, the fibrous tissue band separating inner and outer muscularis propria, the outer muscularis propria and finally the serosa and serosal fat. The ultrasonographic visualization of these additional layers has however not yet been proven helpful in clinical diagnostics.

As an ultrasound pulse propagates through tissue, it interacts with the tissue itself through 3 potential interactions: absorption, scattering, reflection and refraction.^{33, 35} Scattering and reflection are the two main components leading to the ultrasonographic image formation. Reflection occurs when ultrasonographic echoes are generated by specular

reflectors, at the interface of large structures relative to the wavelength of the ultrasonographic pulse, with different acoustic impedance, while scattering occurs when the ultrasound pulse interacts with particles that are similar or smaller than the wavelength of the ultrasound pulse and have different impedance values than the propagating medium.¹³

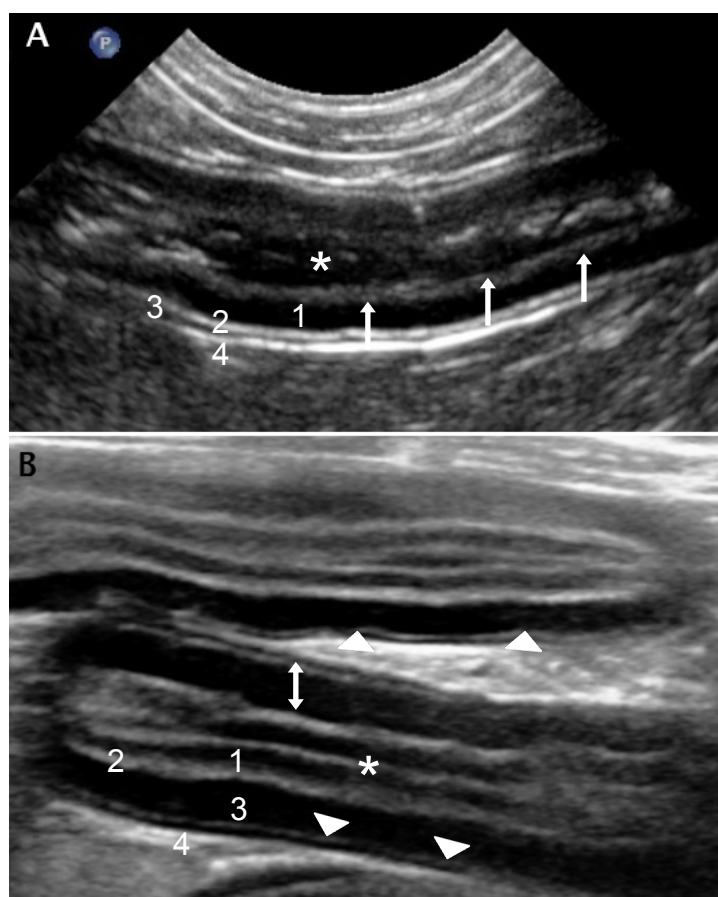


Figure 26 - Examples of additional intestinal layers observed in clinical veterinary patients. (A) Longitudinal image of the duodenum of a dog showing severe hyperechogenicity of the inner mucosa (white single arrowhead lines), similar to the findings observed in our study with intestinal samples having lacteal dilation on histology. This dog had no gastrointestinal clinical signs. The intestinal lumen (white asterisk) is mildly dilated with fluid. (B) Transverse image of the jejunum of a cat diagnosed with eosinophilic enteritis. The thin interface hyperechoic line (white arrowheads) within the thickened muscularis layer (3) (white double arrowhead lines), between the inner and outer muscularis propria layer can be observed in this image, similarly to the findings observed in our study. The intestinal lumen (white asterisk) is empty. (1) Mucosa; (2) submucosa; (3) muscularis propria; (4) serosa.

Scattering is responsible for creating the echogenic texture of the tissue layer. For instance, histological layers containing a large amount of collagen and fat, such as the submucosa, are very reflective and scatter ultrasound to a greater degree than other tissues, therefore explaining their hyperechogenicity on the ultrasonographic images. According to the physical principles previously discussed, it is then considered likely that the difference of

organization of the intestinal villi compared to the lamina propria, as well as their different histological tissue composition, would explain the difference of echogenicity observed between these two regions of the mucosa on our ultrasonographic images. Similarly, the presence of dilated lacteals in some of our intestinal samples would explain the hyperechoic inner area observed in the epithelium of these samples (Figure 23), as dilated lacteals contain dietary fats, which are very reflective and strongly scatter ultrasound.⁶⁰ This hyperechoic inner mucosal area has been observed by the authors in clinical cases (Figure 26A) in dogs that did not have any intestinal clinical signs of disease. The clinical significance of this ultrasonographic finding remains unclear. It is however the authors' impression that this finding is different from the previously reported hyperechoic mucosal striations described in association with lymphangiectasia in dogs.¹⁰ The distribution of these hyperechoic striations in dogs with confirmed lymphangiectasia is not identical when compared to the echogenic mucosal lining seen in our study. Furthermore, in that same previous study,¹⁰ concurrent inflammation was a commonly associated feature of lacteal dilation and lymphangiectasia, with a mild-to-moderate mucosal inflammatory infiltration present in 91% of the dogs. Interestingly, during clinical work, this hyperechoic mucosal area also seems to be observed more commonly in small intestinal segments that have a mild luminal dilation (as seen on the Figure 26A). Therefore in our population, we suspect that this hyperechoic mucosal lining could simply represent a normal post-prandial finding, and correspond to trapped gas/echogenic chyme between the epithelial villi associated with mild dilation of the lacteals, as it has been previously reported that oral administration of corn oil or a fatty meal may induce/increase lacteal dilation in healthy dogs and dogs with lymphangiectasia, and accentuate the ultrasonographic visualization of small intestinal lacteals.⁶⁰ Interestingly one of our dogs did not have lacteal dilation on histology, despite visualization of the same hyperechoic mucosal lining ultrasonographically. A similar finding was reported in the previous lymphangiectasia study,¹⁰ where one dog had hyperechoic mucosal striations visualized ultrasonographically, despite lack of lacteal dilation histopathologically. The reason for this finding in both this previous study and ours is unknown, and one can only speculate

that it may be the result of a sampling error/alteration or ultrasound artifact, as there were no other histopathological changes otherwise explaining the ultrasonographic findings.

An additional thin hyperechoic mucosal line running parallel to the submucosa was also observed in the ileal samples of four of the dogs of our study. A similar hyperechoic mucosal line has been previously reported in both dogs and cats.^{60, 63} In a study of 11 cats,⁶³ this hyperechoic line has been correlated histologically with small intestinal mucosal fibrosis. In that study,⁶³ it was mainly observed within the jejunum compared to the duodenum, but was not reported in the ileum of the 11 cats included. A similar echoic mucosal line has also been reported more recently in dogs.⁶⁰ In this recent study, following oral administration of corn oil, a mucosal hyperechoic line running parallel to the submucosa became visible in the duodenum and jejunum of healthy dogs and dogs diagnosed with lymphangiectasia and was assumed to represent a dilated lymphatic vessel, responsible for uptake of fat from the lacteals, becoming more conspicuous after corn oil administration because of its distension.⁶⁰ However, despite the transient feature of this ultrasound finding, which made a lymphatic dilation a possible source, this assumption was not confirmed histologically. In our study, in the ileal samples where this line was observed, there was no evidence of dilated lymphatic vessels histologically and only the enlarged submucosal lymphoid follicles (Peyer's patches) differed from the other intestinal samples lacking this hyperechoic thin mucosal line. Similarly, in our samples there was no histological evidence of mucosal fibrosis, as previously demonstrated in cats,⁶³ and this line was also only seen in the ileal samples in our study, while it was not reported in the ileum of the 11 cats included in the mucosal fibrosis study.⁶³ This finding in dogs could therefore be secondary to the lymphoid tissue distribution within the gastrointestinal tract. The gut-associated lymphoid tissue (GALT) in the small intestine mainly consist of lymphoid nodules, including Peyer's patches, isolated lymphoid follicles, cryptopatches, and lymphocytes within the lamina propria and epithelium.¹⁹ The Peyer's patches are located in the intestinal mucosa, extend into the submucosa of the small intestine, and are constituted of aggregated lymphatic cells, forming lymphoid follicles.¹⁹ In dogs, a total of 26–29 Peyer's patches are described, with two different types reported,

depending on their location.^{19, 21} In the jejunum and proximal ileum, the canine Peyer's patches are smaller and more discrete, while a larger Peyer's patch, completely encircling the distal ileum, is present within the distal terminal ileum.¹⁹⁻²¹ This heterogeneous distribution of the Peyer's patches within the small intestinal tract may explain the inconsistent visualization of this hyperechoic mucosal line among our samples, as well as the disparity of its visualization within the ileal samples themselves, maybe due to a difference in localization (more proximal or distal) of the harvesting site of the ileal intestinal samples between our dogs. Mild lymphoid hyperplasia likely represents a response to non-significant immune stimulus; therefore the clinical significance of this line, if observed ultrasonographically in clinical cases, would be unknown. As for now the authors have not seen it in clinical patients, but its observation in dogs would likely be considered a non-significant ultrasonographic feature.

The most consistent finding in our study was the thin hyperechoic line observed within the muscularis propria (Figure 24), which was observed in every small intestinal sample. Compared to the histological samples and similar to what has been described in human medicine,^{12, 14-16, 39} this line is considered to represent the interface between the inner and outer parts of the muscularis propria layer. It is commonly observed in clinical patients, both dogs and cats (Figure 26B), in healthy animals as well, and is considered an incidental finding without any clinical significance.

In our study we also concluded that there were no significant statistical differences between the histological and ultrasonographic small intestinal layer thicknesses. In contrast to our results, in humans, the intestinal layered structure thicknesses seen on ultrasound have been proven to not directly correspond with the intestinal layers seen on histology.^{12, 13} This lack of correlation has been predominantly attributed to the ultrasonographic axial resolution, which is mainly determined by the spatial pulse length (SPL) of the transducer, itself determined by the frequency and damping characteristics of the ultrasound probe.^{16, 33, 35} Although the interface between two intestinal layers may have no thickness histologically, the hyperechoic interface echoes produced between the two layers will be at least the same thickness as the spatial pulse length.^{13, 16, 33, 35} If the layer beyond this interface is

hypoechoic compared to the layer superficial to the same interface, then the superficial layered structure and the interface echo will be merged on the ultrasonographic image and the superficial layer will appear thicker than it actually is, while the hypoechoic layer beyond the interface will appear thinner (Figure 27A).^{13, 16, 33, 35} If the intestinal layer beyond this interface is hypoechoic compared to the layer superficial to the interface, and the layer beyond the interface is thinner than the spatial pulse length, then the hypoechoic layer beyond this interface will be obscured by the hyperechoic echo from the interface and will not be visualized on the ultrasound image (Figure 27B).^{13, 16, 33, 35} If the layer beyond this interface is hyperechoic compared to the interface, then the interface echo will blend with the echoes from the hyperechoic layer itself and the thickness of the structures will not change (Figure 27C).

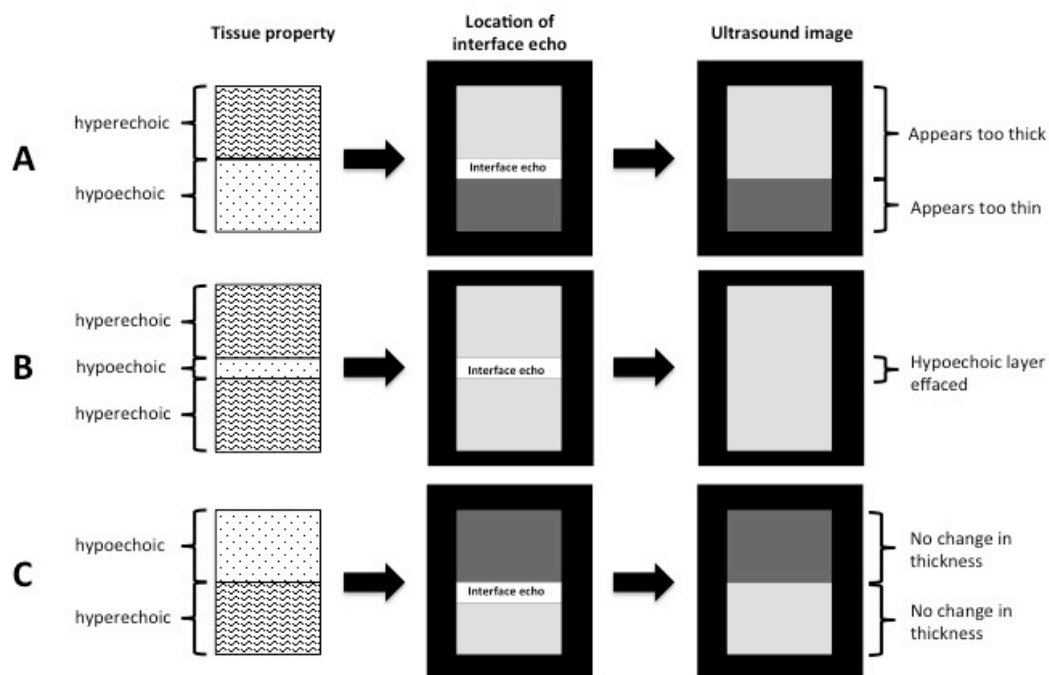


Figure 27 – Effects of interface echoes on ultrasound layering. Depending on the echogenicity of the tissues surrounding an interface, the superficial layer will either look thicker (A) or unchanged (C) on the ultrasound image and a small hypoechoic layer, thinner than the SPL, and surrounded by hyperechoic tissue will be effaced (B), due to the hyperechoic interface formed on the ultrasound image. (Adapted from¹⁶)

This physical principle may explain why there are discrepancies between the intestinal layer thickness on histology and on ultrasound in human medicine, and why some thin layers may not be observed ultrasonographically. Despite the lack of significant statistical

differences between ultrasound and histology in our study, it may also explain why we subjectively observed that the serosal layer appeared thicker on the ultrasound images than it was on histology (Figure 24B and D). A recent study evaluating the thickness of the different small intestinal layers in healthy dogs measured ultrasonographically, reported a serosal thickness within a similar range than the one measured ultrasonographically in our study.¹⁰⁰ In that report,¹⁰⁰ there was no correlation performed with histology. In our study, despite the lack of significant statistical difference, subjectively, there was a 6 to 12 times difference noted between the histological serosal and ultrasonographic serosal measurements. Therefore, it is our impression, that the hyperechoic line observed at the outer aspect of the intestinal sample on ultrasound, and described as the serosal layer itself in most veterinary ultrasonographic textbooks,^{3, 4} is more likely to represent an interface echo, and its thickness to possibly correspond to the spatial pulse length, rather than representing the true thickness of the histological serosa. This is further supported by the lack of reported intestinal disease inducing specific serosal layer thickening on ultrasound and has also been considered in other veterinary studies in healthy cats.¹⁰¹

Further reasons explaining why in our study the histological and ultrasonographic intestinal layers correlate, when they do not in humans, may possibly be related to the histological differences observed between canine and human small intestine. The small intestinal loops in humans appear thinner than they are in dogs (Table 4 and Table 6), ranging between 1 to 3 mm in diameter, depending on the study and degree of dilation of the intestinal lumen,^{25, 27, 44, 94} (up to 2 mm variation between distended and empty intestinal loops) and the different small intestinal layers appear to have a lesser degree of thickness variation compared to the intestinal layers in dogs (Table 7).⁴⁴

Table 6 – Wall thickness in different region of the gastrointestinal tract in 122 healthy persons measured with a 12MHz transducer.

(Adapted from⁴⁴)

Location	Mean \pm SD (mm)
Duodenum	1.6 \pm 0.3
Jejunum	0.9 \pm 0.2
Ileum	1.1 \pm 0.3

Table 7 – Ileal wall layer thickness in 122 healthy persons measured with transabdominal ultrasound.

(Adapted from⁴⁴)

Layer	Mean \pm SD (mm)
Mucosa	0.4 \pm 0.1
Submucosa	0.4 \pm 0.1
Muscularis propria	0.4 \pm 0.2

Finally, other possible reasons that could explain the statistical differences previously reported in human medicine between histological and ultrasonographic layering may be due to the processing of the small intestinal loops after surgical resection. Previous studies have demonstrated disparate results in margins length when intestinal specimens were measured in vivo by the surgeon and ex vivo by the pathologist.^{48, 99, 102} In one study, 5cm long colorectal intestinal samples were resected surgically then measured pre- and post-formalin fixation.⁹⁹ The majority of the organ shrinkage (70%) occurred immediately, within the first minutes after removal of the specimens from the patient, while formalin fixation contributed to only 30% of the intestinal shrinkage. A 40% shrinkage of the length of the intestinal samples was observed prior to fixation, when the resected sample was left in a specimen container for 10 to 20 minutes in an unfixed state, and an overall shrinkage of 57% in length was measured after fixation. In this same study,⁹⁹ prior to formalin fixation, one end of the samples was pinned on a wax board and stretched back to its original length (measured prior to surgical resection), while the other end was left floating freely in formalin. In contrary to the free-floating end of the samples, the pinned halves of the samples almost maintained their original length after fixation. An other study reported a similar average shrinkage of 48% of the resection margins of the intestinal samples after formalin fixation.¹⁰² Furthermore, according to the literature, the thickness of the intestinal samples is expected to vary between 10 and 16% during paraffin embedding and histological sectioning.⁴⁸ This is in agreement with the results of our study. When the intestinal samples were harvested, immediately after resection, the intestinal loops severely contracted, likely due to fiber muscle contraction, as well as blood supply interruption. However, after the intestinal samples were pinned on the paraffin block, their length appeared subjectively unchanged and comparison of the total thickness of

the small intestinal samples pre- and post-formalin fixation did not reveal any significant statistical differences. The variation of intestinal thickness reported in the literature before paraffin embedding of the small intestinal samples and after histological sectioning may also be due to the alteration of the small intestinal samples, that may get crushed during histological sectioning.⁴⁸ In our study, 4 of the 36 intestinal samples had to be recut, as their quality prevented adequate evaluation and measurements of the different histological layers (Figure 19 and Figure 20). The layer most commonly affected was the mucosa, with the epithelium most often involved, most likely due to the fragility of the intestinal epithelial villi.

It is therefore apparent that the length and thickness of a resection specimen changes during several stages from devitalization to the histological section. Consequently, direct comparison of absolute intestinal wall thickness measurements between in vivo and ex vivo intestinal segments will likely be inaccurate, and measurements of small intestinal wall thickness should be used carefully and in conjunction with other more subjective findings, when used for diagnostic purposes.

CONCLUSION

In contrary to what was hypothesized and has been reported in the human literature, our study did not show any significant statistical differences between histological and ultrasonographic layer thicknesses in the small intestine of healthy adult dogs. It is therefore concluded that the small intestinal ultrasonographic and histological layers correlate in dogs. However, as demonstrated with the subjective assessment of the serosal layer, despite the lack of statistical significant difference, it should be kept in mind that direct comparison of absolute intestinal wall thickness measurements between in vivo and ex vivo intestine may still be inaccurate, and that measurements of small intestinal wall thickness should be used carefully and in conjunction with other more subjective findings, when used with a diagnostic purpose.

Additional intestinal layers could also be observed during our ex vivo examination of the small intestine that have not been previously reported in normal dogs. Some of these layers were considered to be physiologic interfaces, such as the interface between the circular and longitudinal muscular fibers of the muscularis layer, while some were correlated with histopathological findings, such as the hyperechoic mucosal lining associated with epithelial mucosal lacteal dilation or the ileal thin hyperechoic line parallel to the submucosa, associated with submucosal lymphoid follicles hyperplasia.

It is our impression that some of these newly described findings are commonly observed in a clinical setting and may be merely associated with improved ultrasonographic transducer technology compared to much earlier reports that utilized the comparatively poorer resolution transducers of that era.

REFERENCES

1. Penninck DG, Nyland TG, Fisher PE, Kerr LY. Ultrasonography of the normal canine gastrointestinal tract. *Vet Radiol*. 1989;**30**: 272-276.
2. Delaney F, O'Brien RT, Waller K. Ultrasound evaluation of small bowel thickness compared to weight in normal dogs. *Vet Radiol Ultrasound*. 2003;**44**: 577-580.
3. Penninck D. Gastrointestinal tract. In: Nyland TG, Mattoon JS (eds): *Small Animal Diagnostic Ultrasound*. Saunders, 2002;207-230.
4. Penninck D. Gastrointestinal tract In: Penninck D, d'Anjou M-A (eds): *Atlas of small animal ultrasonography*. Ames, Iowa: Blackwell Pub., 2008;281-318.
5. Gaschen L. Ultrasonography of small intestinal inflammatory and neoplastic diseases in dogs and cats. *Vet Clin North Am Small Anim Pract*. 2011;**41**: 329-344.
6. Larson MM, Biller DS. Ultrasound of the gastrointestinal tract. *Vet Clin North Am Small Anim Pract*. 2009;**39**: 747-759.
7. Penninck D, Smyers B, Webster CR, Rand W, Moore AS. Diagnostic value of ultrasonography in differentiating enteritis from intestinal neoplasia in dogs. *Vet Radiol Ultrasound*. 2003;**44**: 570-575.
8. Gaschen L, Kircher P, Stussi A, Allenspach K, Gaschen F, Doherr M, et al. Comparison of ultrasonographic findings with clinical activity index (CIBDAI) and diagnosis in dogs with chronic enteropathies. *Vet Radiol Ultrasound*. 2008;**49**: 56-64.
9. Stander N, Wagner WM, Goddard A, Kirberger RM. Ultrasonographic appearance of canine parvoviral enteritis in puppies. *Vet Radiol Ultrasound*. 2010;**51**: 69-74.
10. Sutherland-Smith J, Penninck DG, Keating JH, Webster CR. Ultrasonographic intestinal hyperechoic mucosal striations in dogs are associated with lacteal dilation. *Vet Radiol Ultrasound*. 2007;**48**: 51-57.
11. Rault DN, Besso JG, Boulouha L, Begon D, Ruel Y. Significance of a common extended mucosal interface observed in transverse small intestine sonograms. *Vet Radiol Ultrasound*. 2004;**45**: 177-179.
12. Wiersema MJ, Wiersema LM. High-resolution 25-megahertz ultrasonography of the gastrointestinal wall: histologic correlates. *Gastrointest Endosc*. 1993;**39**: 499-504.
13. Ødegaard S, Kimmey MB. Location of the muscularis mucosae on high frequency gastrointestinal ultrasound images. *Eur J Ultrasound*. 1994;**1**: 39-50.
14. Byrne MF, Jowell PS. Gastrointestinal imaging: endoscopic ultrasound. *Gastroenterology*. 2002;**122**: 1631-1648.
15. Ødegaard S, Nesje LB, Lærum OD, Kimmey MB. High-frequency ultrasonographic imaging of the gastrointestinal wall. *Expert Rev Med Devices*. 2012;**9**: 263-273.
16. Kimmey MB, Ha Hwang J. Assessment of the Layered Structure of the Gastrointestinal Tract In: Ødegaard S, Helge Gilja O, Gregersen H (eds): *Basic And New Aspects Of Gastrointestinal Ultrasonography*. London, UK: World Scientific Pub Co Inc 2005;167-188.
17. Bacha WJ. Digestive system. In: Bacha WJ, Bacha LM (eds): *Color Atlas of Veterinary Histology*, 2012;139-182.

18. Banks WJ. Digestive system I – Alimentary canal. In: Banks WJ (ed): *Applied Veterinary Histology*. St. Louis, MO, USA: Mosby, 1993;350–353.
19. Cesta MF. Normal structure, function, and histology of mucosa-associated lymphoid tissue. *Toxicol Pathol*. 2006;**34**: 599-608.
20. Haley PJ. Species differences in the structure and function of the immune system. *Toxicology*. 2003;**188**: 49-71.
21. Hogen Esch H, Hahn FF. The lymphoid organs: anatomy, development, and age-related changes. In: Mohr U, Carlton WW, Dungworth DL, Benjamin SA, Capen CC, Hahn FF (eds): *Pathobiology of the Aging Dog*. Ames, Iowa: Iowa State University Press, 2001;127–135.
22. Uchida K, Kamikawa Y. Muscularis mucosae - the forgotten sibling. *J Smooth Muscle Res*. 2007;**43**: 157-177.
23. Greenwood B, Davison JS. The relationship between gastrointestinal motility and secretion. *Am J Physiol*. 1987;**252**: G1-7.
24. Kimmey MB, Martin RW, Haggitt RC, Wang KY, Franklin DW, Silverstein FE. Histologic correlates of gastrointestinal ultrasound images. *Gastroenterology*. 1989;**96**: 433-441.
25. Silverstein F, Kimmey M, Martin R, Haggitt R, Mack L, Moss A, et al. Ultrasound and the intestinal wall: experimental methods. *Scand J Gastroenterol Suppl*. 1986;**123**: 34-40.
26. Spear R, Kimmey MB, Wang KY, Sillery JK, Benjamin DR, Sawin RS. Appendiceal US scans: histologic correlation. *Radiology*. 1992;**183**: 831-834.
27. Haber HP, Stern M. Intestinal ultrasonography in children and young adults: bowel wall thickness is age dependent. *J Ultrasound Med*. 2000;**19**: 315-321.
28. Miller JH, Kemberling CR. Ultrasound scanning of the gastrointestinal tract in children: subject review. *Radiology*. 1984;**152**: 671-677.
29. Paulsen DB, Buddington KK, Buddington RK. Dimensions and histologic characteristics of the small intestine of dogs during postnatal development. *Am J Vet Res*. 2003;**64**: 618-626.
30. Sarria R, Latorre R, Henroteaux M, Henroteaux N, Soria F, Perez-Cuadrado E, et al. Morphometric study of the layers of the canine small intestine at five sampling sites. *Vet J*. 2012;**192**: 498-502.
31. Baum B, Meneses F, Kleinschmidt S, Nolte I, Hewicker-Trautwein M. Age-related histomorphologic changes in the canine gastrointestinal tract: a histologic and immunohistologic study. *World J Gastroenterol*. 2007;**13**: 152-157.
32. Wang L, Li J, Li Q, Zhang J, Duan XL. Morphological changes of cell proliferation and apoptosis in rat jejunal mucosa at different ages. *World J Gastroenterol*. 2003;**9**: 2060-2064.
33. Bushberg JT, Seibert JA, Leidholdt Jr. EM, Boone JM. Ultrasound. *The essential physics of medical imaging*. Philadelphia, PA: Lippincott Williams & Wilkins, 2012;500-576.
34. Nyland TG, Mattoon JS, Herrgesell EJ, Wisner ER. Physical principles, instrumentation, and safety of diagnostic ultrasound. In: Nyland TG, Mattoon JS (eds): *Small Animal Diagnostic Ultrasound*. Saunders, 2002;1-19.

35. Hangiandreou NJ. AAPM/RSNA physics tutorial for residents. Topics in US: B-mode US: basic concepts and new technology. *Radiographics*. 2003;**23**: 1019-1033.
36. Dussik KT, Fritch DJ, Kyriazidou M, Sear RS. Measurements of articular tissues with ultrasound. *Am J Phys Med*. 1958;**37**: 160-165.
37. Zhang J, Rose JL, Shung KK. A computer model for simulating ultrasonic scattering in biological tissues with high scatterer concentration. *Ultrasound Med Biol*. 1994;**20**: 903-913.
38. Sporea I, Popescu A. Ultrasound examination of the normal gastrointestinal tract. *Med Ultrason*. 2010;**12**: 349-352.
39. Aibe T, Fuji T, Okita K, Takemoto T. A fundamental study of normal layer structure of the gastrointestinal wall visualized by endoscopic ultrasonography. *Scand J Gastroenterol Suppl*. 1986;**123**: 6-15.
40. Bolondi L, Caletti G, Casanova P, Villanacci V, Grigioni W, Labo G. Problems and variations in the interpretation of the ultrasound feature of the normal upper and lower GI tract wall. *Scand J Gastroenterol Suppl*. 1986;**123**: 16-26.
41. Bolondi L, Casanova P, Santi V, Caletti G, Barbara L, Labo G. The sonographic appearance of the normal gastric wall: an in vitro study. *Ultrasound Med Biol*. 1986;**12**: 991-998.
42. Caletti GC, Bolondi L, Zani L, Labo G. Technique of endoscopic ultrasonography investigation: esophagus, stomach and duodenum. *Scand J Gastroenterol Suppl*. 1986;**123**: 1-5.
43. Machi J, Takeda J, Sigel B, Kakegawa T. Normal stomach wall and gastric cancer: evaluation with high-resolution operative US. *Radiology*. 1986;**159**: 85-87.
44. Nylund K, Hausken T, Odegaard S, Eide GE, Gilja OH. Gastrointestinal wall thickness measured with transabdominal ultrasonography and its relationship to demographic factors in healthy subjects. *Ultraschall Med*. 2012;**33**: E225-232.
45. Stringer DA, Daneman A, Brunelle F, Ward K, Martin DJ. Sonography of the normal and abnormal stomach (excluding hypertrophic pyloric stenosis in children. *J Ultrasound Med*. 1986;**5**: 183-188.
46. Tio TL, Tytgat GN. Endoscopic ultrasonography of normal and pathologic upper gastrointestinal wall structure. Comparison of studies in vivo and in vitro with histology. *Scand J Gastroenterol Suppl*. 1986;**123**: 27-33.
47. Role of endoscopic ultrasonography. American Society for Gastrointestinal Endoscopy. *Gastrointest Endosc*. 2000;**52**: 852-859.
48. Nylund K, Leh S, Immervoll H, Matre K, Skarstein A, Hausken T, et al. Crohn's disease: Comparison of in vitro ultrasonographic images and histology. *Scand J Gastroentero*. 2008;**43**: 719-726.
49. Graham JP, Newell SM, Roberts GD, Lester NV. Ultrasonographic features of canine gastrointestinal pythiosis. *Vet Radiol Ultrasound*. 2000;**41**: 273-277.
50. Meunier PC, Cooper BJ, Appel MJ, Lanieu ME, Slauson DO. Pathogenesis of canine parvovirus enteritis: sequential virus distribution and passive immunization studies. *Vet Pathol*. 1985;**22**: 617-624.
51. Meunier PC, Cooper BJ, Appel MJ, Slauson DO. Pathogenesis of canine parvovirus enteritis: the importance of viremia. *Vet Pathol*. 1985;**22**: 60-71.

52. Rudolf H, van Schaik G, O'Brien RT, Brown PJ, Barr FJ, Hall EJ. Ultrasonographic evaluation of the thickness of the small intestinal wall in dogs with inflammatory bowel disease. *J Small Anim Pract.* 2005;**46**: 322-326.
53. Penninck DG, Nyland TG, Kerr LY, Fisher PE. Ultrasonographic evaluation of gastrointestinal diseases in small animals. *Vet Radiol.* 1990;**31**: 134-141.
54. Haber HP, Busch A, Ziebach R, Dette S, Ruck P, Stern M. Ultrasonographic findings correspond to clinical, endoscopic, and histologic findings in inflammatory bowel disease and other enterocolitides. *J Ultrasound Med.* 2002;**21**: 375-382.
55. Haber HP, Busch A, Ziebach R, Stern M. Bowel wall thickness measured by ultrasound as a marker of Crohn's disease activity in children. *Lancet.* 2000;**355**: 1239-1240.
56. Ledermann HP, Borner N, Strunk H, Bongartz G, Zollikofer C, Stuckmann G. Bowel wall thickening on transabdominal sonography. *Am J Roentgenol.* 2000;**174**: 107-117.
57. Siegel MJ, Friedland JA, Hildebolt CF. Bowel wall thickening in children: differentiation with US. *Radiology.* 1997;**203**: 631-635.
58. Maconi G, Parente F, Bollani S, Cesana B, Bianchi Porro G. Abdominal ultrasound in the assessment of extent and activity of Crohn's disease: clinical significance and implication of bowel wall thickening. *Am J Gastroenterol.* 1996;**91**: 1604-1609.
59. Kull PA, Hess RS, Craig LE, Saunders HM, Washabau RJ. Clinical, clinicopathologic, radiographic, and ultrasonographic characteristics of intestinal lymphangiectasia in dogs: 17 cases (1996-1998). *J Am Vet Med Assoc.* 2001;**219**: 197-202.
60. Pollard RE, Johnson EG, Pesavento PA, Baker TW, Cannon AB, Kass PH, et al. Effects of corn oil administered orally on conspicuity of ultrasonographic small intestinal lesions in dogs with lymphangiectasia. *Vet Radiol Ultrasound.* 2013;**54**: 390-397.
61. Louvet A, Denis B. Ultrasonographic diagnosis--small bowel lymphangiectasia in a dog. *Vet Radiol Ultrasound.* 2004;**45**: 565-567.
62. Kleinschmidt S, Harder J, Nolte I, Marsilio S, Hewicker-Trautwein M. Chronic inflammatory and non-inflammatory diseases of the gastrointestinal tract in cats: diagnostic advantages of full-thickness intestinal and extraintestinal biopsies. *J Feline Med Surg.* 2010;**12**: 97-103.
63. Penninck DG, Webster CR, Keating JH. The sonographic appearance of intestinal mucosal fibrosis in cats. *Vet Radiol Ultrasound.* 2010;**51**: 458-461.
64. Baez JL, Hendrick MJ, Walker LM, Washabau RJ. Radiographic, ultrasonographic, and endoscopic findings in cats with inflammatory bowel disease of the stomach and small intestine: 33 cases (1990-1997). *J Am Vet Med Assoc.* 1999;**215**: 349-354.
65. Dennis JS, Kruger JM, Mullaney TP. Lymphocytic/plasmacytic colitis in cats: 14 cases (1985-1990). *J Am Vet Med Assoc.* 1993;**202**: 313-318.
66. Nelson RW, Dimperio ME, Long GG. Lymphocytic-plasmacytic colitis in the cat. *J Am Vet Med Assoc.* 1984;**184**: 1133-1135.
67. Al-Haddad S, Riddell RH. The role of eosinophils in inflammatory bowel disease. *Gut.* 2005;**54**: 1674-1675.
68. Weissman A, Penninck D, Webster C, Hecht S, Keating J, Craig LE. Ultrasonographic and clinicopathological features of feline gastrointestinal eosinophilic sclerosing fibroplasia in four cats. *J Feline Med Surg.* 2013;**15**: 148-154.

69. Gaschen L, Granger LA, Oubre O, Gaschen FP. The effect of diet on intestinal mucosal echogenicity in healthy dogs. Annual Phi Zeta Research Day, Louisiana State University School of Veterinary Medicine, Baton Rouge, LA September 24, 2014; Poster.
70. Frisoli JK, Desser TS, Jeffrey RB. Thickened submucosal layer: a sonographic sign of acute gastrointestinal abnormality representing submucosal edema or hemorrhage. *Am J Roentgenol*. 2000;**175**: 1595-1599.
71. Clautice-Engle T, Jeffrey RB, Jr., Li KC, Barth RA. Power Doppler imaging of focal lesions of the gastrointestinal tract: comparison with conventional color Doppler imaging. *J Ultrasound Med*. 1996;**15**: 63-66.
72. Jeffrey RB, Jr., Sommer FG, Debatin JF. Color Doppler sonography of focal gastrointestinal lesions: initial clinical experience. *J Ultrasound Med*. 1994;**13**: 473-478.
73. Fabrick C, Bugbee A, Fosgate G. Clinical features and outcome of *Heterobilharzia americana* infection in dogs. *J Vet Intern Med*. 2010;**24**: 140-144.
74. Kvitko-White HL, Sayre RS, Corapi WV, Spaulding KA. Imaging diagnosis-heterobilharzia americana infection in a dog. *Vet Radiol Ultrasound*. 2011;**52**: 538-541.
75. Barrs VR, Beatty JA. Feline alimentary lymphoma: 1. Classification, risk factors, clinical signs and non-invasive diagnostics. *J Feline Med Surg*. 2012;**14**: 182-190.
76. Daniaux LA, Laurenson MP, Marks SL, Moore PF, Taylor SL, Chen RX, et al. Ultrasonographic thickening of the muscularis propria in feline small intestinal small cell T-cell lymphoma and inflammatory bowel disease. *J Feline Med Surg*. 2014;**16**: 89-98.
77. Laurenson MP, Skorupski KA, Moore PF, Zwingenberger AL. Ultrasonography of intestinal mast cell tumors in the cat. *Vet Radiol Ultrasound*. 2011;**52**: 330-334.
78. Tucker S, Penninck DG, Keating JH, Webster CR. Clinicopathological and ultrasonographic features of cats with eosinophilic enteritis. *J Feline Med Surg*. 2014;**16**: 950-956.
79. Zwingenberger AL, Marks SL, Baker TW, Moore PF. Ultrasonographic evaluation of the muscularis propria in cats with diffuse small intestinal lymphoma or inflammatory bowel disease. *J Vet Intern Med*. 2010;**24**: 289-292.
80. Dechant JE, Whitcomb MB, Magdesian KG. Ultrasonographic diagnosis--idiopathic muscular hypertrophy of the small intestine in a miniature horse. *Vet Radiol Ultrasound*. 2008;**49**: 300-302.
81. Diana A, Pietra M, Guglielmini C, Boari A, Bettini G, Cipone M. Ultrasonographic and pathologic features of intestinal smooth muscle hypertrophy in four cats. *Vet Radiol Ultrasound*. 2003;**44**: 566-569.
82. Bettini G, Muracchini M, Della Salda L, Preziosi R, Morini M, Guglielmini C, et al. Hypertrophy of intestinal smooth muscle in cats. *Res Vet Sci*. 2003;**75**: 43-53.
83. Carreras JK, Goldschmidt M, Lamb M, McLear RC, Drobatz KJ, Sorenmo KU. Feline epitheliotropic intestinal malignant lymphoma: 10 cases (1997-2000). *J Vet Intern Med*. 2003;**17**: 326-331.
84. Lingard AE, Briscoe K, Beatty JA, Moore AS, Crowley AM, Krockenberger M, et al. Low-grade alimentary lymphoma: clinicopathological findings and response to treatment in 17 cases. *J Feline Med Surg*. 2009;**11**: 692-700.
85. Russell KJ, Beatty JA, Dhand N, Gunew M, Lingard AE, Baral RM, et al. Feline low-grade alimentary lymphoma: how common is it? *J Feline Med Surg*. 2012;**14**: 910-912.

86. Briscoe KA, Krockenberger M, Beatty JA, Crowley A, Dennis MM, Canfield PJ, et al. Histopathological and immunohistochemical evaluation of 53 cases of feline lymphoplasmacytic enteritis and low-grade alimentary lymphoma. *J Comp Pathol.* 2011;**145**: 187-198.
87. Waly NE, Gruffydd-Jones TJ, Stokes CR, Day MJ. Immunohistochemical diagnosis of alimentary lymphomas and severe intestinal inflammation in cats. *J Comp Pathol.* 2005;**133**: 253-260.
88. Moore PF, Woo JC, Vernau W, Kosten S, Graham PS. Characterization of feline T cell receptor gamma (TCRG) variable region genes for the molecular diagnosis of feline intestinal T cell lymphoma. *Vet Immunol Immunopathol.* 2005;**106**: 167-178.
89. Gabella G. Hypertrophy of intestinal smooth muscle. *Cell Tissue Res.* 1975;**163**: 199-214.
90. Chaffin MK, Fuenteabla IC, Schumacher J, Welch RD, Edwards JF. Idiopathic muscular hypertrophy of the equine small intestine: 11 cases (1980-1991). *Equine Vet J.* 1992;**24**: 372-378.
91. Cordes DO, Dewes HF. Diverticulosis and muscular hypertrophy of the small intestine of horses, pigs and sheep. *N Z Vet J.* 1971;**19**: 108-111.
92. Brehmer A, Gobel D, Frieser M, Graf M, Radespiel-Troger M, Neuhuber W. Experimental hypertrophy of myenteric neurones in the pig: a morphometric study. *Neurogastroenterol Motil.* 2000;**12**: 155-162.
93. Gabella G. Hypertrophic smooth muscle. I. Size and shape of cells, occurrence of mitoses. *Cell Tissue Res.* 1979;**201**: 63-78.
94. Fleischer AC, Muhletaler CA, James AE, Jr. Sonographic assessment of the bowel wall. *Am J Roentgenol.* 1981;**136**: 887-891.
95. Murata Y, Napoleon B, Odegaard S. High-frequency endoscopic ultrasonography in the evaluation of superficial esophageal cancer. *Endoscopy.* 2003;**35**: 429-436.
96. Strohm WD, Classen M. Benign lesions of the upper GI tract by means of endoscopic ultrasonography. *Scand J Gastroenterol Suppl.* 1986;**123**: 41-46.
97. Boscaini M, Moscini PL, Montori A. Transrectal ultrasonography: interpretation of normal intestinal wall structure for the preoperative staging of rectal cancer. *Scand J Gastroenterol Suppl.* 1986;**123**: 87-98.
98. Odegaard S, Kimmey MB, Martin RW, Yee HC, Cheung AH, Silverstein FE. The effects of applied pressure on the thickness, layers, and echogenicity of gastrointestinal wall ultrasound images. *Gastrointest Endosc.* 1992;**38**: 351-356.
99. Goldstein NS, Soman A, Sacksner J. Disparate surgical margin lengths of colorectal resection specimens between in vivo and in vitro measurements. The effects of surgical resection and formalin fixation on organ shrinkage. *Am J Clin Pathol.* 1999;**111**: 349-351.
100. Gladwin NE, Penninck DG, Webster CR. Ultrasonographic evaluation of the thickness of the wall layers in the intestinal tract of dogs. *Am J Vet Res.* 2014;**75**: 349-353.
101. Di Donato P, Penninck D, Pietra M, Cipone M, Diana A. Ultrasonographic measurement of the relative thickness of intestinal wall layers in clinically healthy cats. *J Feline Med Surg.* 2014;**16**: 333-339.
102. Weese JL, O'Grady MG, Ottery FD. How long is the five centimeter margin? *Surg Gynecol Obstet.* 1986;**163**: 101-103.

APPENDIX – PERMISSIONS TO USE COPYRIGHTED MATERIAL

15/3/2015

Rightslink Printable License

JOHN WILEY AND SONS LICENSE TERMS AND CONDITIONS

Mar 15, 2015

This Agreement between Alexandre Le Roux ("You") and John Wiley and Sons ("John Wiley and Sons") consists of your license details and the terms and conditions provided by John Wiley and Sons and Copyright Clearance Center.

License Number	3590421411692
License date	Mar 15, 2015
Licensed Content Publisher	John Wiley and Sons
Licensed Content Publication	Veterinary Radiology & Ultrasound
Licensed Content Title	ULTRASONOGRAPHIC APPEARANCE OF CANINE PARVOVIRAL ENTERITIS IN PUPPIES
Licensed Content Author	NERISSA STANDER,WENCKE M. WAGNER,AMELIA GODDARD,ROBERT M. KIRBERGER
Licensed Content Date	Jan 4, 2010
Pages	6
Type of use	Dissertation/Thesis
Requestor type	University/Academic
Format	Print and electronic
Portion	Figure/table
Number of figures/tables	2
Original Wiley figure/table number(s)	Figure 2 Figure 4
Will you be translating?	No
Title of your thesis / dissertation	CORRELATION OF ULTRASONOGRAPHIC SMALL INTESTINAL WALL LAYERING WITH HISTOLOGY IN NORMAL DOGS
Expected completion date	Apr 2015
Expected size (number of pages)	70
Requestor Location	Alexandre Le Roux The Animal Medical Center 510 East 62nd Street NEW YORK, NY 10065 United States Attn: Alexandre Le Roux
Billing Type	Invoice
Billing Address	Alexandre Le Roux The Animal Medical Center 510 East 62nd Street NEW YORK, NY 10065 United States Attn: Alexandre Le Roux
Total	0.00 USD

<https://s100.copyright.com/App/PrintableLicenseFrame.jsp?publisherID=140&publisherName=Wiley&publication=VRU&publicationID=29027&rightID=1&ty...> 1/6

JOHN WILEY AND SONS LICENSE TERMS AND CONDITIONS

Mar 15, 2015

This Agreement between Alexandre Le Roux ("You") and John Wiley and Sons ("John Wiley and Sons") consists of your license details and the terms and conditions provided by John Wiley and Sons and Copyright Clearance Center.

License Number	3590421004846
License date	Mar 15, 2015
Licensed Content Publisher	John Wiley and Sons
Licensed Content Publication	Veterinary Radiology & Ultrasound
Licensed Content Title	EFFECTS OF CORN OIL ADMINISTERED ORALLY ON CONSPICUITY OF ULTRASONOGRAPHIC SMALL INTESTINAL LESIONS IN DOGS WITH LYMPHANGIECTASIA
Licensed Content Author	Rachel E. Pollard, Eric G. Johnson, Patricia A. Pesavento, Tomas W. Baker, Allison B. Cannon, Philip H. Kass, Stanley L. Marks
Licensed Content Date	Mar 18, 2013
Pages	8
Type of use	Dissertation/Thesis
Requestor type	University/Academic
Format	Print and electronic
Portion	Figure/table
Number of figures/tables	2
Original Wiley figure/table number(s)	Figure 4 Figure 5
Will you be translating?	No
Title of your thesis / dissertation	CORRELATION OF ULTRASONOGRAPHIC SMALL INTESTINAL WALL LAYERING WITH HISTOLOGY IN NORMAL DOGS
Expected completion date	Apr 2015
Expected size (number of pages)	70
Requestor Location	Alexandre Le Roux The Animal Medical Center 510 East 62nd Street NEW YORK, NY 10065 United States Attn: Alexandre Le Roux
Billing Type	Invoice
Billing Address	Alexandre Le Roux The Animal Medical Center 510 East 62nd Street NEW YORK, NY 10065 United States Attn: Alexandre Le Roux

VITA

Alexandre Benjamin Le Roux was born in Pontoise next to Paris, in France in March 1981. After a Degree in Life Science at the University of Paris XI, France, he began his veterinary education at the National Veterinary School of Nantes, France in 2002. After receiving his Veterinary Degree in 2006, Dr. Le Roux completed a one-year small animal rotating internship at the National Veterinary School of Toulouse, France, followed by a one-year diagnostic imaging internship at the Veterinary School of Liege, in Belgium.

In 2009, Dr. Le Roux moved to Baton Rouge for a four-year residency in diagnostic imaging at the Louisiana State University School of Veterinary Medicine, USA. He completed his residency in July 2013 and became board-certified from the European College of Veterinary Diagnostic Imaging in 2012 and from the American College of Veterinary Radiology in 2014.

Dr. Le Roux is currently working as a staff veterinary radiologist at the Animal Medical Center, in New York City, USA.